

Making Images Real Again: A Comprehensive Survey on Deep Image Composition

Li Niu*, Wenyan Cong, Liu Liu, Yan Hong, Bo Zhang, Jing Liang, Liqing Zhang

Abstract—As a common image editing operation, image composition aims to combine the foreground from one image and another background image, resulting in a composite image. However, there are many issues that could make the composite images unrealistic. These issues can be summarized as the inconsistency between foreground and background, which includes appearance inconsistency (e.g., incompatible illumination), geometry inconsistency (e.g., unreasonable size), and semantic inconsistency (e.g., mismatched semantic context). Image composition task could be decomposed into multiple sub-tasks, in which each sub-task targets at one or more issues. Specifically, object placement aims to find reasonable scale, location, and shape for the foreground. Image blending aims to address the unnatural boundary between foreground and background. Image harmonization aims to adjust the illumination statistics of foreground. Shadow generation aims to generate plausible shadow for the foreground. These sub-tasks can be executed sequentially or parallelly to acquire realistic composite images. To the best of our knowledge, there is no previous survey on image composition. In this paper, we conduct comprehensive survey over the sub-tasks and combinatorial task of image composition. For each one, we summarize the existing methods, available datasets, and common evaluation metrics. Datasets and codes for image composition are summarized at <https://github.com/bcml/Awesome-Image-Composition>.

I. INTRODUCTION

During image composition, we combine the foreground from one image and another background image to form a composite image. More generally, image composition can be used for combining multiple visual elements from different sources to construct a new image. After compositing a new image with foreground and background, there exist many issues that could make the composite image unrealistic and thus significantly degrade its quality. These issues can be summarized as the inconsistency between foreground and background, which can be divided into appearance inconsistency, geometric inconsistency, and semantic inconsistency. Each type of inconsistency involves a number of issues to be solved. Image composition task could be decomposed into multiple sub-tasks, in which each sub-task targets at one or more issues. Next, we will introduce each type of inconsistency one by one.

The appearance inconsistency is including but not limited to: 1) unnatural boundary between foreground and background; 2) incompatible illumination statistics between foreground and background; 3) missing or implausible shadow and reflection of foreground; 4) resolution, sharpness, and noise

Li Niu, Wenyan Cong, Liu Liu, Yan Hong, Bo Zhang, Jing Liang, and Liqing Zhang are with MOE Key Lab of Artificial Intelligence, Department of Computer Science and Engineering Shanghai Jiao Tong University, Shanghai, China (email: {ustcnewl,plcwyam17320,shirley,Hy2628982280,bo-zhang,leungjing,lqzhang}@sjtu.edu.cn).

* means the corresponding author.



Fig. 1. Image composition aims to combine the foreground object and the background image to generate a realistic composite image.

discrepancy between foreground and background [78]. For the first issue, the foreground is usually extracted using image segmentation [104] or matting [166, 32] algorithms. However, the foregrounds may not be precisely delineated, especially at the boundaries. When pasting the foreground with jagged boundaries on the background, there would be obvious color artifacts along the boundary. To solve this issue, image blending [159, 180] aims to address the unnatural boundary between foreground and background, so that the foreground could be seamlessly blended with the background. For the second issue, since the foreground and background may be captured in different conditions (e.g., weather, season, time of the day, camera setting), the obtained composite image could be inharmonious (e.g., foreground captured in the daytime and background captured at night). To solve this issue, image harmonization [146, 21, 17] aims to adjust the illumination statistics of foreground to make it more compatible with the background, so that the whole image looks more harmonious. For the third issue, when pasting the foreground on the background, the foreground may also affect the background with shadow or reflection. To solve this issue, shadow generation [91, 184, 126] or reflection generation [102] focus on generating plausible shadow or reflection for the foreground according to both foreground and background information. As far as we are concerned, there are only few works [102] on generating reflection for the inserted object probably due to the limited application scenarios, so we focus on shadow generation in this paper. For the fourth issue, the foreground and background may be from two images with different resolutions, blur degrees, and noise patterns. The resolution (*resp.*, sharpness, noise) discrepancy between them could be mitigated by using super-resolution [156], deblurring [178], denoising [143] techniques.

The geometric inconsistency is including but not limited to: 1) the foreground object is too large or too small; 2) the foreground object does not have reasonable supporting force (e.g., hanging in the air); 3) unreasonable occlusion; 4)

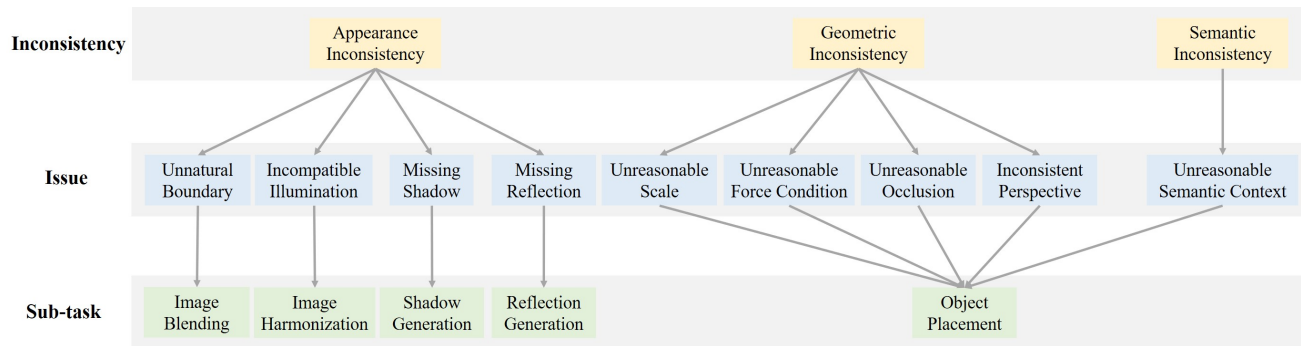


Fig. 2. The quality of composite image is degraded by the appearance inconsistency, geometric inconsistency, and semantic inconsistency. Each type of inconsistency involves a number of issues. Each sub-task targets at addressing one or more issues.

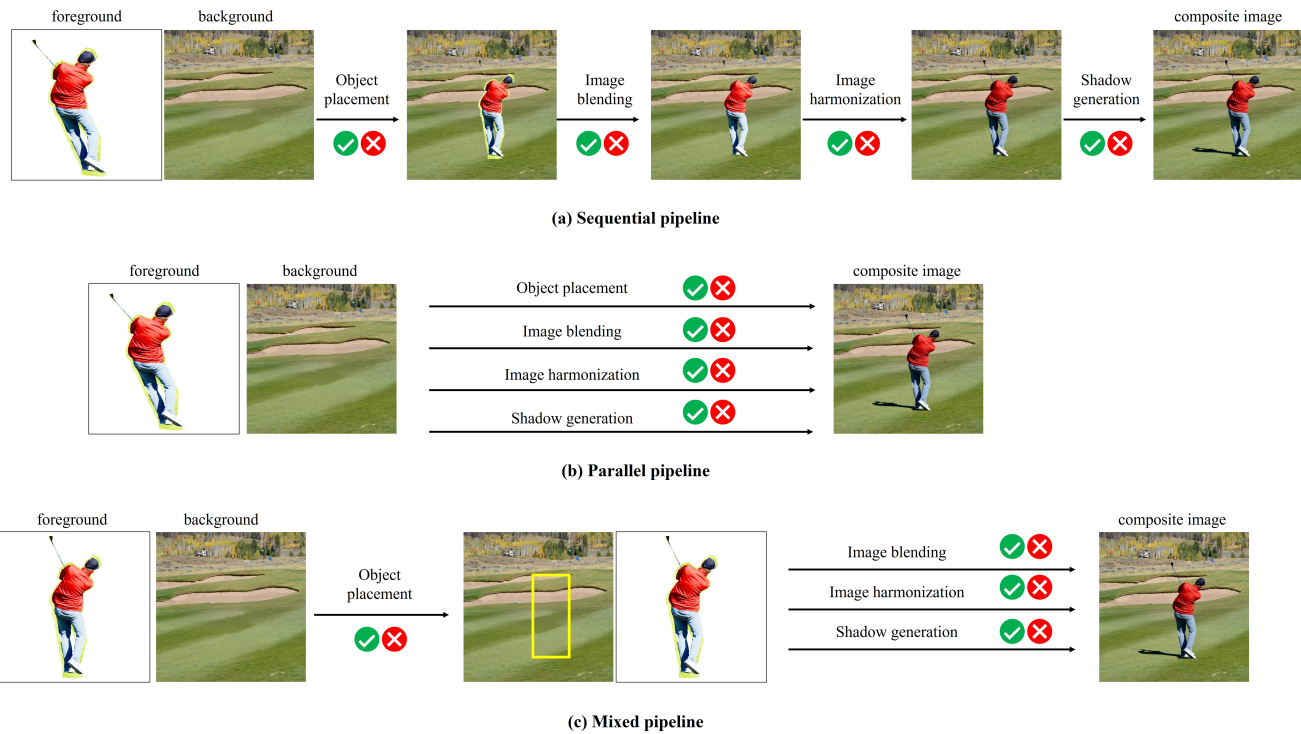


Fig. 3. Previous works perform multiple sub-tasks (e.g., object placement, image blending, image harmonization, shadow generation) sequentially or parallelly to achieve the goal of image composition.

inconsistent perspectives between foreground and background. In summary, the location, size, and shape of the foreground may be irrational considering the geometric constraints. Object placement [2, 23, 65, 144, 179] tends to seek for reasonable location, size, and shape by predicting the foreground transformation to avoid the abovementioned inconsistencies. Previous object placement methods [179, 144] mainly predict simple form of spatial transformation, that is, shifting and scaling the foreground to achieve reasonable location and size. Some other methods [65, 87] predict more general form of spatial transformation (e.g., affine transformation, perspective transformation, thin plate spline transformation) to warp the foreground. In terms of more advanced geometric transformation like view synthesis, we should resort to generative approaches [169, 132] to change the viewpoint of the foreground. When placing the

object on the background, unreasonable occlusion may occur. Most previous methods seek for reasonable placement to avoid unreasonable occlusions, while some methods [2, 174, 137] aim to fix unreasonable occlusion by removing the occluded regions of foreground based on the estimated depth information.

The semantic inconsistency is including but not limited to: 1) the foreground appears at a semantically unreasonable place (e.g., a zebra is placed in the living room); 2) the foreground has unreasonable interactions with other objects or people (e.g., a person is riding a motorbike, but the person and the motorbike are facing towards opposite directions). The semantic inconsistency is judged based on commonsense knowledge, so the cases of semantic inconsistency may be arguable according to subjective judgement. For example,

TABLE I

THE ISSUES TO BE SOLVED IN IMAGE COMPOSITION TASK AND THE CORRESPONDING DEEP LEARNING METHODS TO SOLVE THESE ISSUE. NOTE THAT SOME METHODS ONLY FOCUS ON ONE ISSUE WHILE SOME METHODS ATTEMPT TO SOLVE MULTIPLE ISSUES SIMULTANEOUSLY. “BOUNDARY” MEANS REFINING THE BOUNDARY BETWEEN FOREGROUND AND BACKGROUND. “APPEARANCE” MEANS ADJUSTING THE ILLUMINATION OF FOREGROUND. “SHADOW” MEANS GENERATING SHADOW FOR THE FOREGROUND. “GEOMETRY” MEANS SEEKING FOR REASONABLE LOCATION, SIZE, AND SHAPE FOR THE FOREGROUND CONSIDERING GEOMETRIC CONSTRAINTS. “OCCLUSION” MEANS COPING WITH THE UNREASONABLE OCCLUSION. “SEMANTICS” MEANS FINDING SUITABLE SEMANTIC CONTEXT FOR THE OBJECT.

boundary	appearance	shadow	geometry	occlusion	semantics	methods
+						[176]
	+					[146, 21, 17, 18, 47, 130, 43, 89, 158, 53, 85, 193, 59, 46, 42, 19, 147, 167, 119, 64, 41, 151, 95, 99, 136, 60, 13, 125, 108, 107]
+	+					[159, 180, 164]
	+		+		+	[172]
	+	+				[173, 3]
		+				[91, 184, 55, 50, 103]
			+		+	[23, 65, 87, 135, 144, 179, 81, 80, 93, 106, 24, 149, 192, 183]
			+	+	+	[2, 174]
				+		[137]
+	+		+		+	[12]
+	+	.	.		+	[169, 132, 186, 15]

when a car is placed in the water, it can be argued that a car is sinking into the water after a car accident. However, such event has rather low probability compared with commonly seen cases, so we can claim that the car appears at an unreasonable place, which belongs to semantic inconsistency. The solution to semantic inconsistency often falls into the scope of object placement. To be exact, by predicting suitable spatial transformation for the foreground, we can relocate the foreground to a reasonable place or adjust the pose of foreground to make its interactions with environment more convincing. Therefore, object placement assumes the duty of addressing geometric inconsistency and semantic inconsistency simultaneously.

So far, we have introduced several sub-tasks (*e.g.*, image blending, image harmonization, shadow generation, object placement), in which one sub-task targets at one or multiple issues. Previous works usually focus on one sub-task or perform multiple sub-tasks sequentially (*i.e.*, image blending followed by image harmonization) as shown in Fig. 3(a). The reasonable sequential order is as follows. Given a pair of foreground and background, we first use object placement to find suitable scale and location for the foreground, and use image blending to refine the boundary between foreground and background. Then, we use image harmonization to adjust the foreground illumination and shadow generation to generate plausible shadow for the foreground. Recently, as the diffusion models have demonstrated unprecedented generation ability, some works [169, 132] utilize diffusion models to perform multiple sub-tasks (*e.g.*, image blending, image harmonization, view synthesis) parallelly as shown in the right part of Fig. 3(c). Given a pair of foreground and background with bounding box, they propose one unified model to directly produce the composite image, in which the foreground is blended seamlessly and harmoniously into the background.

These methods re-generate the foreground object instead of making restrained adjustments for the foreground object, so we refer to them as generative image composition methods. We summarize all the potential issues and the corresponding methods to solve them in Table I. In the last row, we use \cdot instead of $+$ for “shadow” and “geometry”, because the shadow and geometry issues are only partially solved, which will be explained in Section VI.

Instead of creating realistic composite images from arbitrary pairs of foregrounds and backgrounds, another solution is seeking for suitable foregrounds from a foreground library, which are compatible with the background in terms of illumination, geometry, and semantics. Finding compatible foregrounds can greatly alleviate the burden of creating realistic composite images, which is complementary with the aforementioned image composition techniques. This task is called foreground object search [191, 162, 75], which is especially useful when we have a high-quality foreground library with wide coverage.

Image composition has a broad spectrum of applications in the realm of entertainment, virtual reality, artistic creation, E-commerce [12, 158, 185] and data augmentation [25, 118, 109] for downstream tasks. For example, people can replace the backgrounds of self-portraits and make the obtained images more realistic using image composition techniques [147, 164]. Similar application scenarios include virtual conference room or virtual card room. Another example is artistic creation, in which image composition can be used to create fantastic artworks that originally only exist in the imagination. Moreover, image composition could also be used for automatic advertising, which helps advertisers with the product insertion in the background scene [185]. When the product is clothes or furniture, this application scenario is also known as virtual try-

on or virtual home decoration [87]. Similarly, advertisement logo compositing [80] targets at embedding some specified logos in target images. The obtained composite images can be taken as design renderings or blueprint to help the designer and the client choose their preferable versions. Additionally, image composition could create synthetic composite images with close data distribution to real images, to augment the training data for downstream tasks like object detection and instance segmentation [25, 118, 109].

In the remainder of this paper, we will elaborate on each sub-task or combinatorial task. In particular, we will introduce object placement in Section II, image blending in Section III, image harmonization in Section IV, shadow generation in Section V, generative image composition in Section VI, foreground object search in Section VII. In each section, we will introduce the existing methods, available datasets, and common evaluation metrics. Finally, we will conclude the whole paper in Section VIII. The contributions of this paper can be summarized as follows,

- To the best of our knowledge, this is the first comprehensive survey on deep image composition.
- We summarize the issues in image composition as three types of inconsistencies. We clarify the relation between inconsistency, issue, sub-task, and pipeline in Fig. 2. We also summarize the issues that previous works attempt to solve in Table I. All the above summaries give rise to a large picture for deep image composition.
- For each sub-task and combinatorial task, we survey the existing methods, available datasets, and common evaluation metrics. We believe that this comprehensive survey can serve as the roadmap for the future research in a broad community.

II. OBJECT PLACEMENT

Object placement aims to paste the foreground on the background with suitable location, size, and shape. As shown in Fig. 4, the cases of unreasonable object placement are including but not limited to: a) the foreground object has inappropriate size (*e.g.*, the dog is too large); b) the foreground object has unreasonable occlusion with background objects (*e.g.*, the fences are unreasonably occluded by the giraffe); c) the foreground object does not have reasonable force condition (*e.g.*, the suitcase is floating in the air); d) the foreground object appears at a semantically unreasonable place (*e.g.*, the boat appears on the land); e) inconsistent perspectives between foreground and background (*e.g.*, the car and the bus have inconsistent perspectives). By taking all the above factors into consideration, object placement is a very challenging task.

A. Traditional Methods

Some object placement methods design explicit rules to find reasonable location and scale for the foreground object. For example, Remez et al. [118] proposed to move the foreground object of fixed scale along the same horizontal scanline on the background. They assume that the locations along the same horizontal scanline have similar depth, so that the true scale of foreground object can be well-preserved.

Wang et al. [150] designed the instance-switching strategy to generate new images through switching different instances of the same class with similar shape and scale. To better refine the position where the object is pasted, Fang et al. [28] explored appearance consistency heatmap to guide the object placement, based on the intuition that an object could be moved to another location which has similar visual context to its original visual context. Specifically, one element in the appearance consistency heatmap measures the similarity between the visual context at this point and original visual context. Georgakis et al. [38] proposed to combine support surface detection and semantic segmentation to find proper location for placing the object. With the determined location, the size of the object is decided in the light of the depth at this location and the original scale of the object. Zhang et al. [185] proposed to model the probability distribution of bounding box information conditioned on background image and foreground category using Gaussian mixture model.

Although these rules are effective in some cases, they are incomplete and sometimes inaccurate, which is far below the requirement to handle the diverse and complicated challenges in object placement task.

B. Deep Learning Methods

Apart from the above methods which design explicit rules to infer the reasonable placement for the foreground object, some methods [172, 2, 174, 137, 153] employ deep learning techniques to predict the placement and generate the composite image automatically.

The existing deep learning based object placement methods can be divided into category-specific object placement and instance-specific object placement. For category-specific object placement, the model aims to predict plausible bounding boxes given a background image and a foreground category. This group of methods assume that the predicted bounding boxes are suitable for all instances belonging to the same foreground category. Nevertheless, this assumption is too restrictive, because different instances from the same category may have distinct properties (*e.g.*, geometry, fine-grained semantics) and thus require bounding boxes with different scales/locations. In contrast, instance-specific object placement methods aim to predict plausible spatial transformations given a background image and a specific foreground object. The difference between category-specific object placement and instance-specific object placement is shown in Fig. 5. Next, we will introduce these two groups of works separately.

1) *Category-specific Object Placement*: Category-specific object placement methods can be categorized into generative approach and discriminative approach. The generative approach targets at predicting one or multiple reasonable bounding boxes for the foreground category, whereas the discriminative approach aims to predict the rationality score of a bounding box for certain foreground category. The discriminative approach can be further divided into slow discriminative approach and fast discriminative approach. The slow discriminative approach takes in a background image with foreground bounding box and predicts a rationality score.

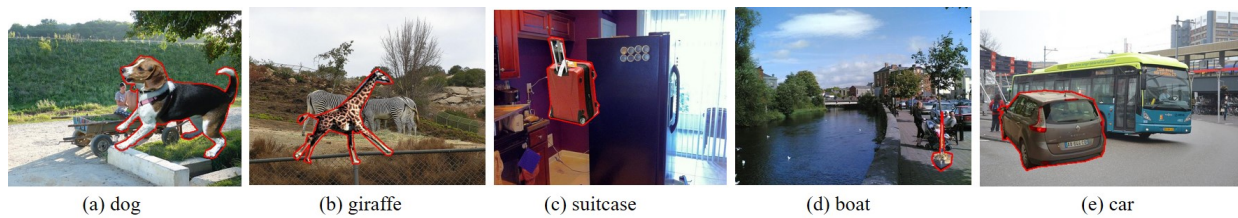


Fig. 4. Examples of unreasonable object placements. The inserted foreground objects are marked with red outlines. From left to right: (a) objects with inappropriate size; (b) unreasonable occlusion; (c) objects hanging in the air; (d) objects appearing at the semantically unreasonable place; (e) inconsistent perspectives.

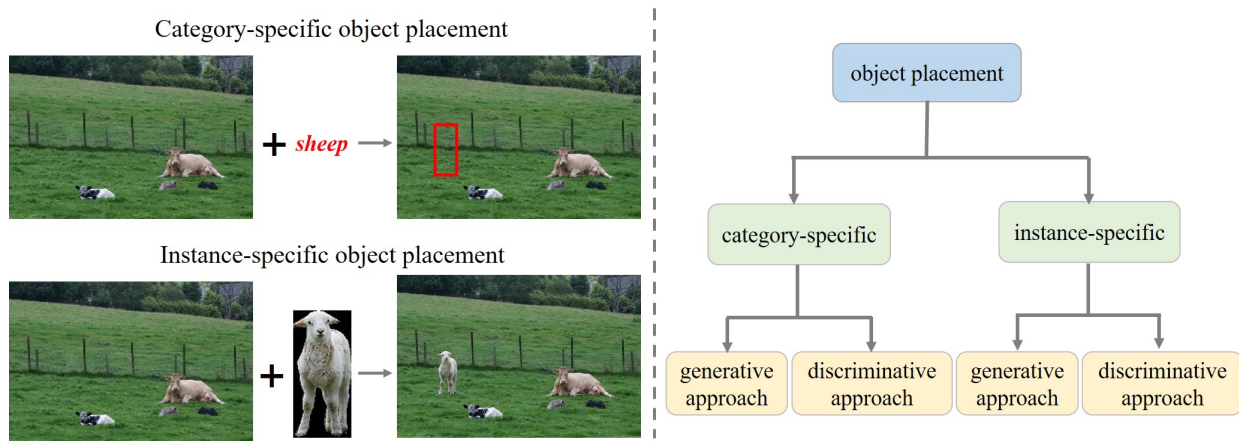


Fig. 5. In the left subfigure, we compare category-specific object placement with instance-specific object placement. In the right subfigure, we show the taxonomy of existing object placement methods.

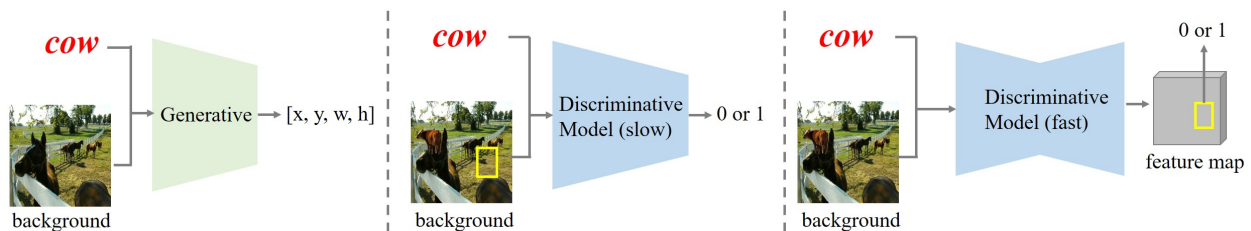


Fig. 6. We show three types of methods for category-specific object placement. *Generative model*: given the foreground category and background image, the model generates a reasonable bounding box (e.g., location (x,y) and scale (w,h)). *Slow discriminative model*: given the foreground category, foreground bounding box, and background image, the model predicts a rationality score. *Fast discriminative model*: given the foreground category and background image, the model uses sliding window on the feature map to get the rationality score for each bounding box.

The fast discriminative approach takes in a background and produces a feature map, based on which sliding window is used to predict the rationality score of each bounding box. The comparison between generative model, slow discriminative model, and fast discriminative model is illustrated in Fig. 6.

Generative approaches: Tan et al. [135] proposed to predict the location and scale of inserted object by taking the background image and object layout as input. Besides, the bounding box prediction task is converted to a classification task by discretizing the locations and scales. Lee et al. [73] investigated on taking a background semantic map instead of a background image as input. Given a background semantic map, they designed a network consisting of two generative modules, in which the first module accounts for the bounding

box of inserted object and the second module accounts for the mask shape of inserted object.

Discriminative approaches: The methods in [23, 24] used a network to predict whether a bounding box is suitable for certain foreground category, based on the contextual information surrounding the bounding box. This approach needs to pass through the network once for each bounding box, which is very time-consuming. To accelerate this process, Volokitin et al. [149] employed masked convolutions to aggregate the contextual information along four directions as context feature maps, based on which the contextual information excluding each bounding box can be obtained efficiently to predict the rationality score for this bounding box.

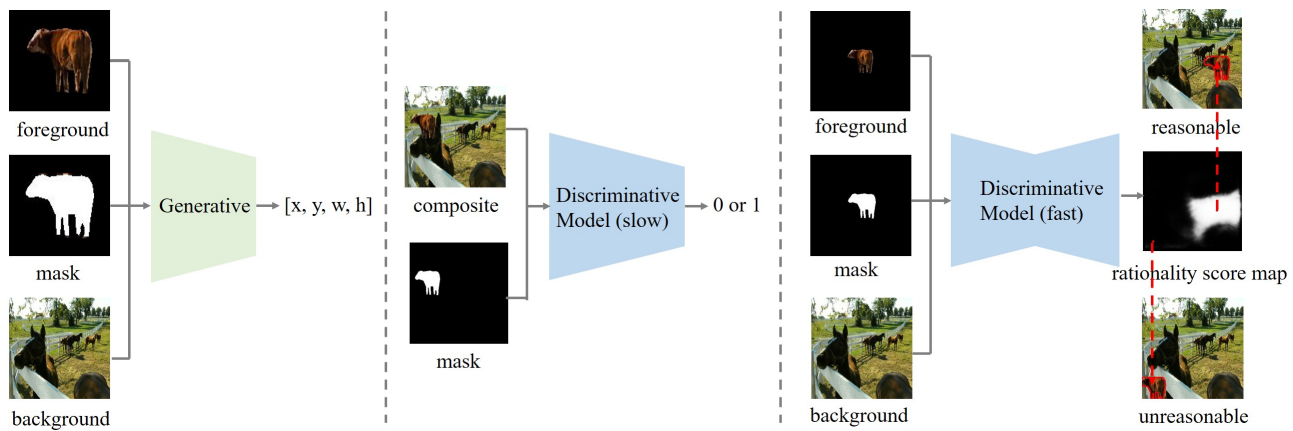


Fig. 7. We show three types of methods for instance-specific object placement. *Generative model*: given the foreground, foreground object mask, and background, the model generates a reasonable placement (e.g., location (x,y) and scale (w,h)) for the foreground. *Slow discriminative model*: given the composite image and composite foreground mask, the model predicts a rationality score. *Fast discriminative model*: given the foreground, foreground object mask, and background, the model predicts a rationality score map containing the rationality scores for all locations.

2) *Instance-specific Object Placement*: Instance-specific object placement methods can also be categorized into generative approach and discriminative approach. The generative approach targets at predicting one or multiple reasonable placements (i.e., spatial transformations) for the foreground object, whereas the discriminative approach aims to predict the rationality score of a composite image in terms of the foreground object placement. The discriminative approach can be further divided into slow discriminative approach and fast discriminative approach. The slow discriminative approach takes in a composite image and predicts a rationality score. The fast discriminative approach takes in a pair of foreground and background, and predicts a rationality score map. The comparison between generative model, slow discriminative model, and fast discriminative model is illustrated in Fig. 7.

Generative approaches: Generative approaches [144, 179, 87, 81, 80] predict different types of spatial transformations (e.g., shifting and scaling, affine transformation, perspective transformation) for the foreground object, which is more flexible and powerful than category-specific object placement methods. For instance, Tripathi et al. [144] developed a model with generator, discriminator, and target network. Given a pair of background and foreground, the generator predicts the affine transformation for the foreground object to produce a composite image. The produced composite image is expected to fool the discriminator and fit the target network corresponding to a downstream task (e.g., object detection). Similarly, Zhan et al. [172] adopted spatial transformer network (STN) [57] to predict the warping parameters under an adversarial learning framework. To produce multiple reasonable placements, Zhang et al. [179] combined the foreground feature, background feature, and a random vector to predict the object placement. Moreover, they ensure the diversity of object placement by enforcing the pairwise distances between predicted placements to approach those between corresponding random vectors. To promote the diversity of generated placements, Zhou et al. [189] established the bijection between random vector and positive composite image. Moreover, they reformulated object

placement as a graph completion task. In particular, background nodes have both content features and placements, while the inserted foreground node only has content feature, giving rise to an incomplete graph. Hence, they estimated the missing placement for the foreground node to complete the graph. Zhang et al. [183] proposed to make sequential decisions to produce a reasonable placement by using reinforcement learning. Azadi et al. [2] employed STN to warp the foreground and relative appearance flow network to change the viewpoint of foreground. Additionally, they investigated on self-consistency constraint, that is, the generated composite image could be decomposed back to the foreground and background. ST-GAN [87] proposed to warp a foreground object into a background image with iterative spatial transformations predicted by STN. As a follow-up work, Kikuchi et al. [65] replaced the iterative spatial transformations in [87] with one-shot spatial transformation.

In terms of view synthesis, some of the above methods [2, 87] predicted geometric transformations (e.g., perspective transformation) to adjust the viewpoint, but the view synthesis ability is quite limited, especially for drastic viewpoint change (e.g., from front view to side view). To accomplish drastic viewpoint change, generative composition methods attempted to re-generate the foreground object, which will be introduced in Section VI.

Discriminative approaches: Liu et al. [93] proposed a discriminative approach named SimOPA to verify whether a composite image is rational in terms of the foreground object placement. Particularly, they feed the concatenation of composite image and foreground mask into a binary classification network to predict a rationality score. However, this discriminative approach is very inefficient, because they need to go through the discriminative network multiple times to find a reasonable object placement. To address this issue, Niu et al. [106] dubbed SimOPA as slow object placement assessment (SOPA) model and proposed a fast object placement assessment (FOPA) model, which can predict the rationality scores at all locations by going through the model only

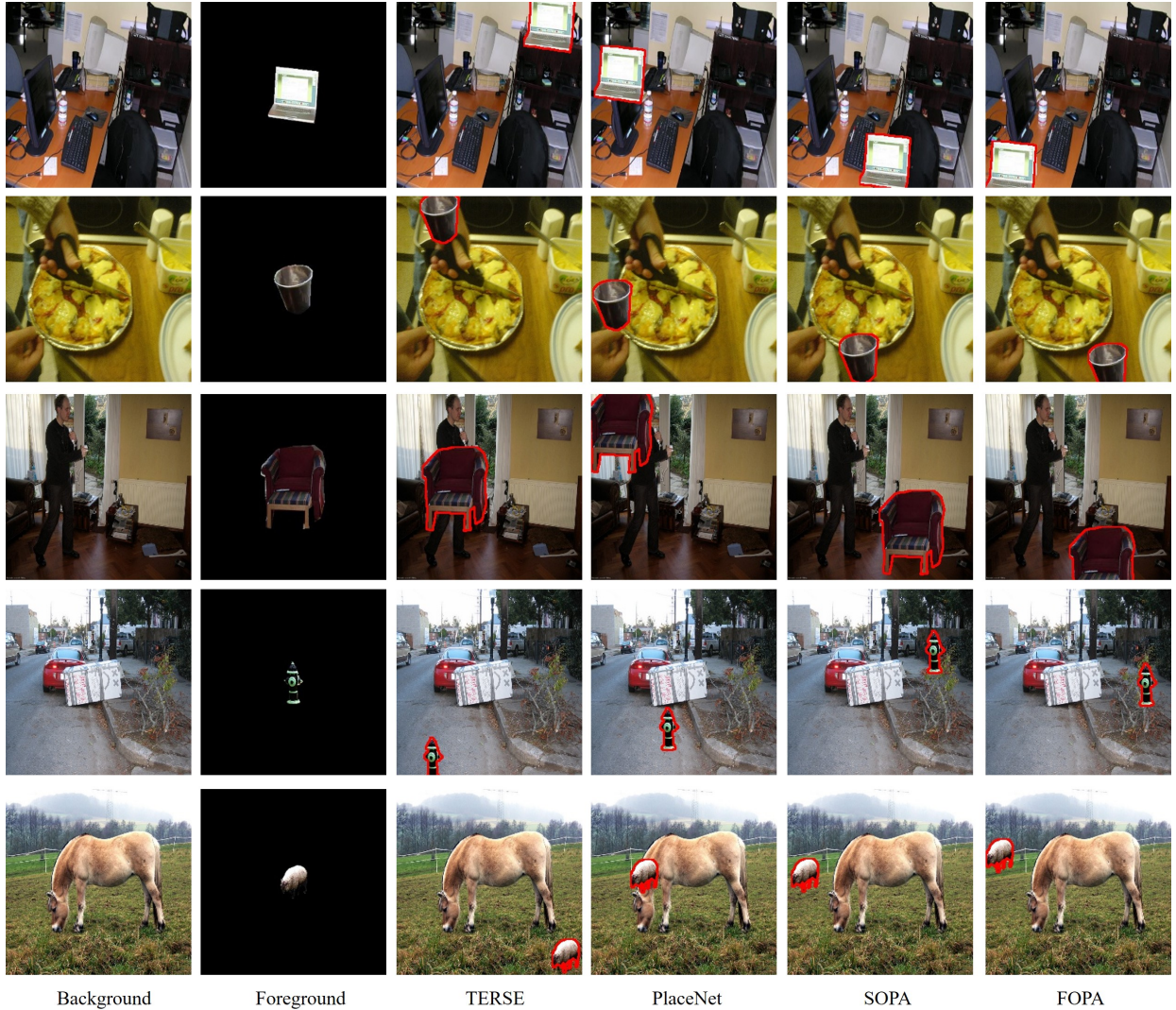


Fig. 8. The visualization results of different object placement methods on OPA dataset [93]. From left to right in each row, we show the foreground, background, and composite images obtained by TERSE [144], PlaceNet [179], SimOPA (SOPA) [93], FOPA [106].

once. Precisely, they take in a pair of background and scaled foreground, and produce a rationality score map, in which each entry represents the rationality score of the composite image obtained by pasting the foreground at this location. They developed several innovations (*e.g.*, background prior transfer, feature mimicking) to bridge the performance gap between FOPA and SOPA, reaching the conclusion that FOPA can achieve comparable performance with SimOPA at significantly reduced cost. FOPA [106] has also demonstrated stronger ability to generate realistic composite images than generative approaches [189, 183]. Similar to FOPA [106], Zhu et al. [192] proposed to predict the rationality scores of all scales and locations, based on the interaction output between foreground and background using transformer [148].

In the end, we briefly discuss the occlusion issue. Most of the above methods seek for reasonable placements to avoid the occurrence of occlusion, *i.e.*, the inserted foreground is not occluded by background objects. Differently, a few methods [2, 174, 137] attempt to address the unreasonable

occlusion when it occurs. Specifically, they first estimate the relative depth relation between the foreground object and the surrounding background objects. Then, they remove the occluded part of foreground object. In this way, they are able to generate composite images with reasonable inter-object occlusions.

C. Datasets and Evaluation Metrics

In some previous works [144, 28], object placement is used as data augmentation strategy to facilitate the downstream tasks (*e.g.*, object detection, instance segmentation). Therefore, they make use of existing object detection and instance segmentation datasets [88, 27, 20, 37]. In particular, the foregrounds are cropped out based on the annotated segmentation masks. After removing the foreground objects, the remaining incomplete background images are restored to complete background images by using image inpainting techniques [170, 92, 171]. In this manner, triplets of foregrounds, backgrounds, and ground-truth composite images can

be obtained. Some other works focus on specific applications like 2D virtual try-on [87, 65, 81] (*e.g.*, placing glasses/hats on human faces) or logo composition [80] (*e.g.*, attaching logo to product image), so they need to collect foregrounds and backgrounds specifically for these applications. More recently, Liu et al. [93] released a large-scale object placement assessment dataset named *OPA*, which consists of 73,470 composite images and their binary rationality labels. *OPA* dataset is constructed by compositing the foregrounds and backgrounds from COCO dataset [88], followed by manually labelling the rationality of obtained composite images. A large number of annotated composite images could greatly facilitate the research on object placement.

To evaluate the quality of generated composite images, previous object placement works usually adopt the following three schemes: 1) Some works measure the similarity between real images and composite images. For example, Tan et al. [135] score the correlation between the distributions of predicted boxes and ground-truth boxes. Zhang et al. [179] calculate Fréchet Inception Distance (FID) [48] between composite images and real images. However, they cannot evaluate each individual composite image. 2) Some works [144, 28] utilize the performance improvement of downstream tasks (*e.g.*, object detection) to evaluate the quality of composite images, where the training sets of the downstream tasks are augmented with generated composite images. However, the evaluation cost is quite huge and the improvement in downstream tasks may not reliably reflect the quality of composite images, because it has been revealed in [39] that randomly generated unrealistic composite images could also boost the performance of downstream tasks. 3) Another common evaluation strategy is user study, where people are asked to score the rationality of object placement [73, 135]. User study complies with human perception and each composite image can be evaluated individually. However, due to the subjectivity of user study, the gauge in different papers may be dramatically different. There is no unified benchmark dataset and the results in different papers cannot be directly compared. 4) Finally, with the recently released *OPA* dataset [93], we could use the annotated composite images for evaluation. Nevertheless, the sparse annotations only cover a small proportion of locations and scales, which limits the universal evaluation of arbitrary composition results.

D. Experiments

In this section, we focus on instance-specific object placement and compare existing object placement methods for generating a reasonable composite image. For ease of comparison, we fix the foreground scale and only predict the reasonable location for the foreground object. Recall that instance-specific object placement methods are divided into generative approaches and discriminative approaches. For generative approach, we choose TERSE [144] and PlaceNet [179], which can directly predict one placement. For discriminative approach, we report the results of SimOPA [93] and FOPA [106]. We use SimOPA and FOPA to generate rationality score map, based on which the location with the largest rationality

score is chosen as the optimal placement. We train and evaluate different methods on *OPA* dataset [93]. The test results are shown in Fig. 8, from which it can be seen that discriminative approaches usually achieve better results than generative approaches. One possible explanation is that TERSE [144] and PlaceNet [179] only utilize the annotated composite images to update the discriminator, without fully using the annotations to train the generator. Nevertheless, discriminative approaches also have failure cases when dealing with occlusion and complex scenes (*e.g.*, unreasonable occlusion between fire hydrant and fallen branches in row 4).

III. IMAGE BLENDING

During image composition, the foreground is usually extracted using image segmentation [104] or matting [166] methods. However, the segmentation or matting results may be noisy and the foregrounds are not precisely delineated. When the foreground with jagged boundaries is pasted on the background, there will be abrupt intensity change between the foreground and background. To refine the boundary and reduce the fuzziness, image blending techniques have been developed.

A. Traditional Methods

Traditional image blending methods aim to smooth the transition between foreground and background. Alpha blending [115] proposed to assign alpha values for boundary pixels indicating what fraction of the colors are from foreground or background, in which the alpha values need to be manually set. Alpha blending is a simple and fast method, but it blurs the fine details and brings in ghost effects. Considering multi-scale information, Laplacian pyramid blending [7] proposed to build multi-scale Laplacian pyramids for two images and perform alpha blending at each scale. Then, the final output is obtained by adding up the blended results of different scales.

Another group of methods attempt to achieve smooth boundary transition by enforcing gradient domain smoothness [30, 63, 74, 134]. The earliest work along this research direction is Poisson image blending [113]. Poisson image blending [113] proposed to enforce the gradient domain consistency with respect to the source image containing the foreground, where the gradient of inserted foreground is computed and propagated from the boundary pixels in the background. Although Poisson image blending can yield more pleasant results than simple alpha blending, it is very time-consuming to solve the Poisson equation. Therefore, there are many follow-up works [134, 138, 63] to accelerate Poisson image blending by using different techniques. Based on the observation that the effectiveness of Poisson image blending seriously depends on the boundary condition, [58] designed a method to optimize the boundary condition. To avoid the color bleeding and halo effect brought by Poisson image blending, Tao et al. [140] developed a two-step algorithm: first processing the gradient values on the boundary and then employing a weighted integration scheme to reconstruct the image from its gradient field.

The above methods based on gradient domain smoothness can smooth the transition between foreground and background

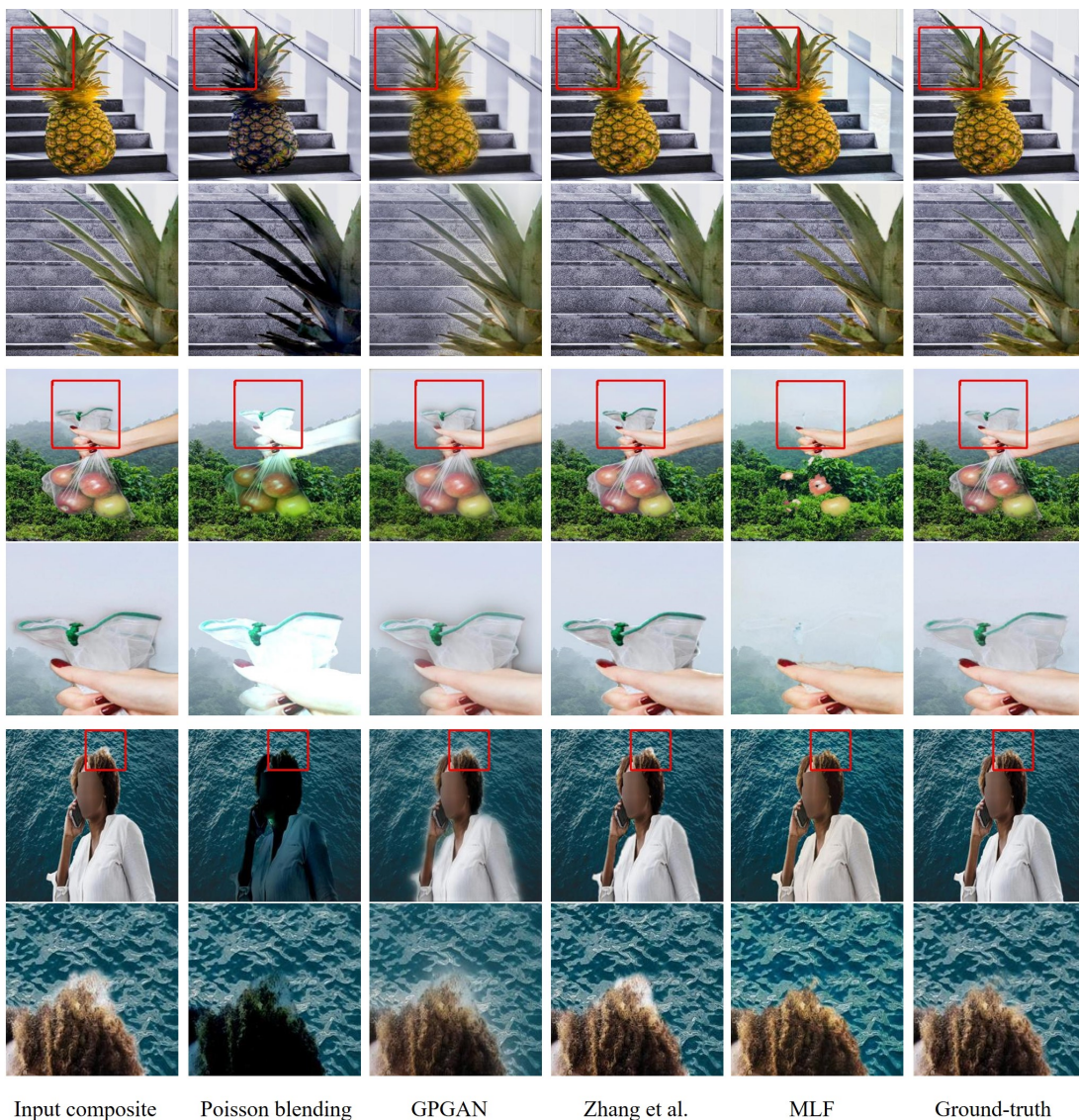


Fig. 9. The leftmost column is the initial composite image obtained using the alpha matte predicted by LFPNet [94]. The rightmost column is the ground-truth composite image obtained using ground-truth alpha matte. The middle columns are the refined results obtained by Poisson image blending [113], GP-GAN [159], Zhang et al. [180], and MLF [176]. The odd rows display the whole image, while the even rows zoom in the red bounding boxes in the odd rows for better observation.

to some extent. However, the colors of background may seep through the foreground too much and distort the foreground color, which would bring significant loss to the foreground content.

B. Deep Learning Methods

Inspired by traditional image blending methods [113, 7], some recent works [159, 180] explored incorporating the function of smoothing boundary into deep learning network. Among them, the works [159, 180, 176] not only enable smooth transition over the boundary, but also reduce the illumination discrepancy between foreground and background, in which the latter one is the goal of image harmonization in Section IV. In this section, we only introduce the way they enable smooth transition over the boundary. These two works [159, 180] are both inspired by [113]. Specifically, they

add the gradient domain constraint to the objective function according to Poisson equation, which can produce a smooth blending boundary with gradient domain consistency. They both optimize over the input composite image to minimize the gradient domain loss. Differently, [159] has a close-form solution, while [180] converts the gradient domain loss to a differentiable loss function and uses gradient descent algorithm.

Different from [159, 180] which are inspired by traditional image blending, recent works [176, 164] proposed learnable image blending, which produces a seamlessly blended image by taking in a pair of foreground image and background image. Specifically, the fusion network in Zhang et al. [176] used two separate encoders to extract and fuse multi-scale features from foreground and background. Because the fusion network relies on ground-truth composite images obtained by using accurate

alpha matte as supervision, the work [176] also proposed an easy-to-hard data-augmentation scheme to relieve the burden of annotating ground-truth alpha matte. Similarly, Xing et al. [164] proposed to concatenate foreground image, background image, and imperfect mask as input to generate a blended image.

C. Datasets and Evaluation Metrics

To the best of our knowledge, there are only few deep learning methods [159, 180, 176] for image blending and there is no unified benchmark dataset. Zhang et al. [180] do not mention the source of used images. Wu et al. [159] manually crop objects from transient attributes database [70] to create input composite images. Similarly, Zhang et al. [176] take foreground images from segmentation datasets [51, 124] and random background images to construct input pairs.

The existing deep image blending works [159, 180, 176] adopt the following evaluation metrics: 1) calculating realism score using the pretrained model [190] which reflects the realism of a composite image; 2) conducting user study by asking engaged users to select the most realistic images; 3) Zhang et al. [176] deem the composite images obtained using ground-truth alpha matte as ground-truth composite image, and calculate Peak Signal-to-Noise Ratio (PSNR) between resultant image and ground-truth composite image.

D. Experiments

We evaluate different image blending methods conditioned on the matting results. First, we create composite images using the alpha mattes predicted by the state-of-the-art trimap-based image matting methods [22, 96, 94]. Then, we hope that image blending methods can refine the obtained composite images. We collect 4500 foreground images from recent image matting datasets [94, 77, 76], which are divided into 4000 for training and 500 for testing. For each foreground image, we randomly select two background images from BG20K [78]. The background images for the training set and test set have no overlap. The training set is used to train the fusion network in MLF [176].

By taking LFPNet [94] as an example matting method, we predict the alpha mattes and obtain the composite images. We observe that LFPNet can generally achieve satisfactory results except some challenging cases. We pick out its several failure cases to verify the effectiveness of image blending methods. We report the results of Poisson image blending [113], GP-GAN [159], Zhang et al. [180], and MLF [176]. We also report the ground-truth composite image obtained using ground-truth alpha matte for comparison. From Fig. 9, it can be seen that the obtained composite images using predicted alpha mattes are very close to the ground-truth composite image except partial boundary regions. We observe that Poisson image blending [113] smooths the transition boundary to some extent, but unexpectedly distorts the foreground content by seeping through the foreground. GP-GAN [159] and Zhang et al. [180] are inspired by Poisson image blending, but use content loss to preserve the original foreground content. Therefore, they strike a balance between preserving the foreground content and

smoothing the boundary. However, some smoothed boundary regions (*e.g.*, hair in the last row) are still not satisfactory. MLF [176] can obtain visually appealing results in some cases. Nonetheless, it may erase detailed information (*e.g.*, the small leaves of pineapple) and fail in handling transparent foreground objects (*e.g.*, plastic bag).

IV. IMAGE HARMONIZATION

Given a composite image, its foreground and background are likely to be captured in different conditions (*e.g.*, weather, season, time of day, camera setting), and thus have distinctive illumination characteristics, which make them look incompatible. Image harmonization aims to adjust the appearance of composite foreground according to composite background to make it compatible with the composite background. We classify the existing methods into rendering based and non-rendering based methods according to whether using rendering techniques.

A. Rendering based Methods

Conventional image relighting [110, 129, 155, 181, 142] aims to adjust the appearance of an image or the object in an image as lit by novel illumination. With some adaptation, image relighting can also be used to adjust the foreground appearance according to the illumination of a new background [110, 181], which bears some resemblance to image harmonization. However, they usually achieve this goal by inferring explicit illumination condition, material properties, and 3D geometry, in which the supervision for these information is difficult and expensive to acquire. Besides, they generally have strong assumption for the light source, which may not generalize well to complicated real-world scenes.

B. Non-rendering based Methods

Early traditional image harmonization methods [168, 133, 71, 131] is performing color transformation for the foreground to match the low-level color statistics between foreground and background. The difference between different methods mainly lies in the matching details. For example, Xue et al. [168] proposed to train a classifier to predict the zone (*e.g.*, low, middle, high) of the histogram which can be best matched between foreground and background, and then adjust the foreground color to match the selected zone between foreground and background. [133] explored decomposing an image into a multi-resolution pyramid with multiple subbands, and performing histogram matching for each subband between foreground and background. Lalonde and Efros [71] proposed to represent foreground and background with color clusters, followed by matching foreground and background color clusters. Song et al. [131] proposed to calculate the color transformation (channel-wise scales) based on gray pixels of foreground and background, because normalized illumination color can be directly derived from the pixel values of gray pixels. In some works on sky replacement [194, 139, 145], they attempted to match the color statistics (*e.g.*, mean, variance) between sky region and non-sky region. Broadly speaking, traditional

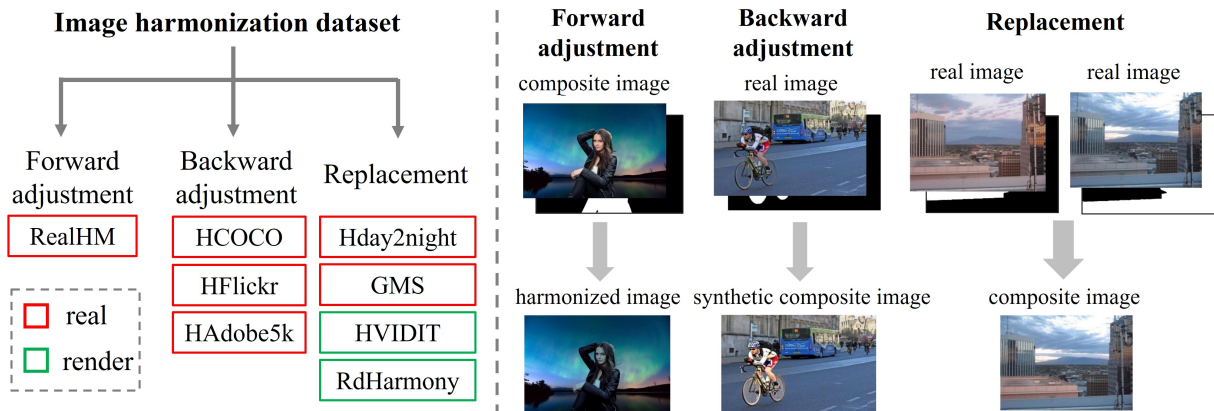


Fig. 10. In the left subfigure, we summarize three ways to construct image harmonization dataset and list the corresponding datasets: RealHM [59], iHarmony4 [9] (HCOCO, HFlicker, HAdobe5k, Hday2night), GMS [131], HVIDIT [43], RdHarmony [9]. We also mark the dataset based on real (*resp.*, rendered) images with red (*resp.*, green) box. In the right subfigure, we provide the illustration of three ways to construct image harmonization dataset.

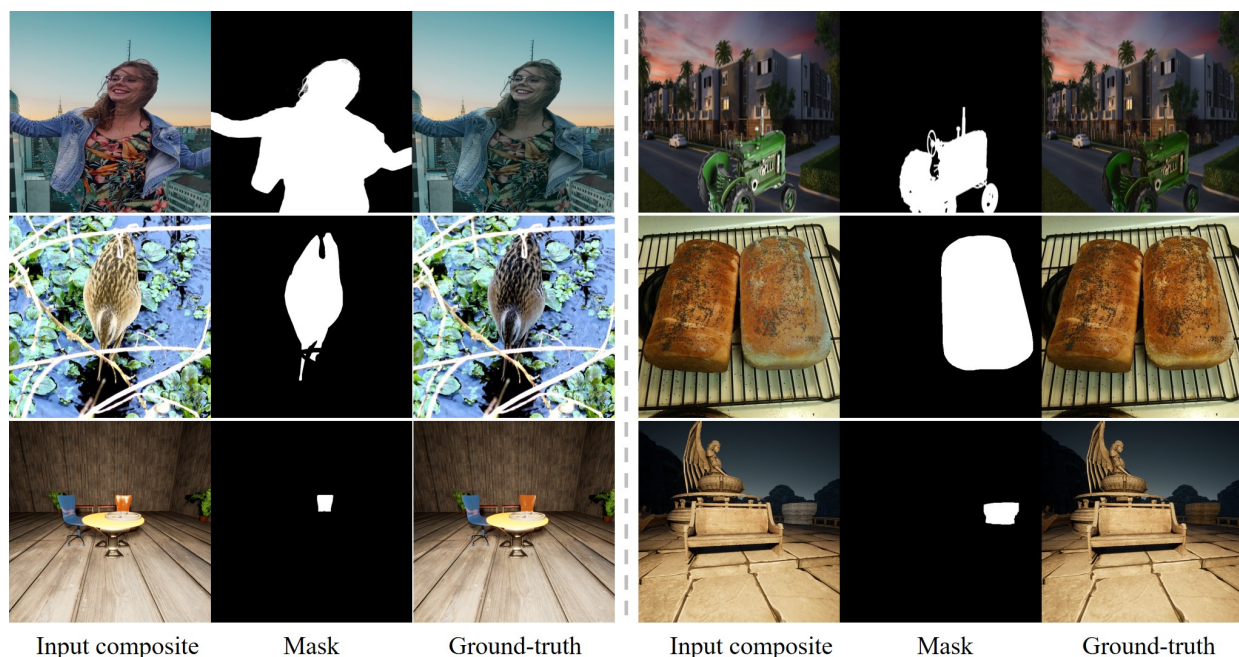


Fig. 11. In the first (*resp.*, second, third) row, we show two examples from RealHM [59] (*resp.*, HFlicker in iHarmony4 [9], HVIDIT [43]) dataset. From left to right in each example, we show the composite image, the foreground mask, and the ground-truth harmonized image.

color transfer methods [117, 163, 31, 114, 29, 1] can also be used for color matching between foreground and background to produce a harmonized image.

Early deep learning based image harmonization methods target at making the harmonized images indistinguishable from real images. For instance, Zhu et al. [190] explored predicting the realism of an image using a CNN classifier. With such realism predictor, they learn the color transformation for the foreground to achieve high realism score, and also enforce the color variation in different channels to be close. Similar to [190], the works [173, 12] used adversarial learning to make the harmonized images indistinguishable from real images. Bhattad and Forsyth [5] drew inspiration from Retinex theory [66] that an image can be decomposed into albedo

(reflectance) and shading (illumination). On the premise of this assumption, an image harmonization model is trained so that the harmonized result should have consistent albedo and consistent background shading with input composite image.

With the emergence of image harmonization datasets consisting of paired training data (see Section IV-E), abundant image harmonization methods [146, 17, 19, 95, 99, 136, 60] using paired supervision have been developed. Tsai et al. [146] proposed the first end-to-end CNN network for image harmonization and leveraged auxiliary semantic segmentation branch to enhance the basic image harmonization network. Another work Sofiiuk et al. [130] also utilized high-level semantic features, which are inserted into the encoder to provide auxiliary information. Cun and Pun [21] designed an

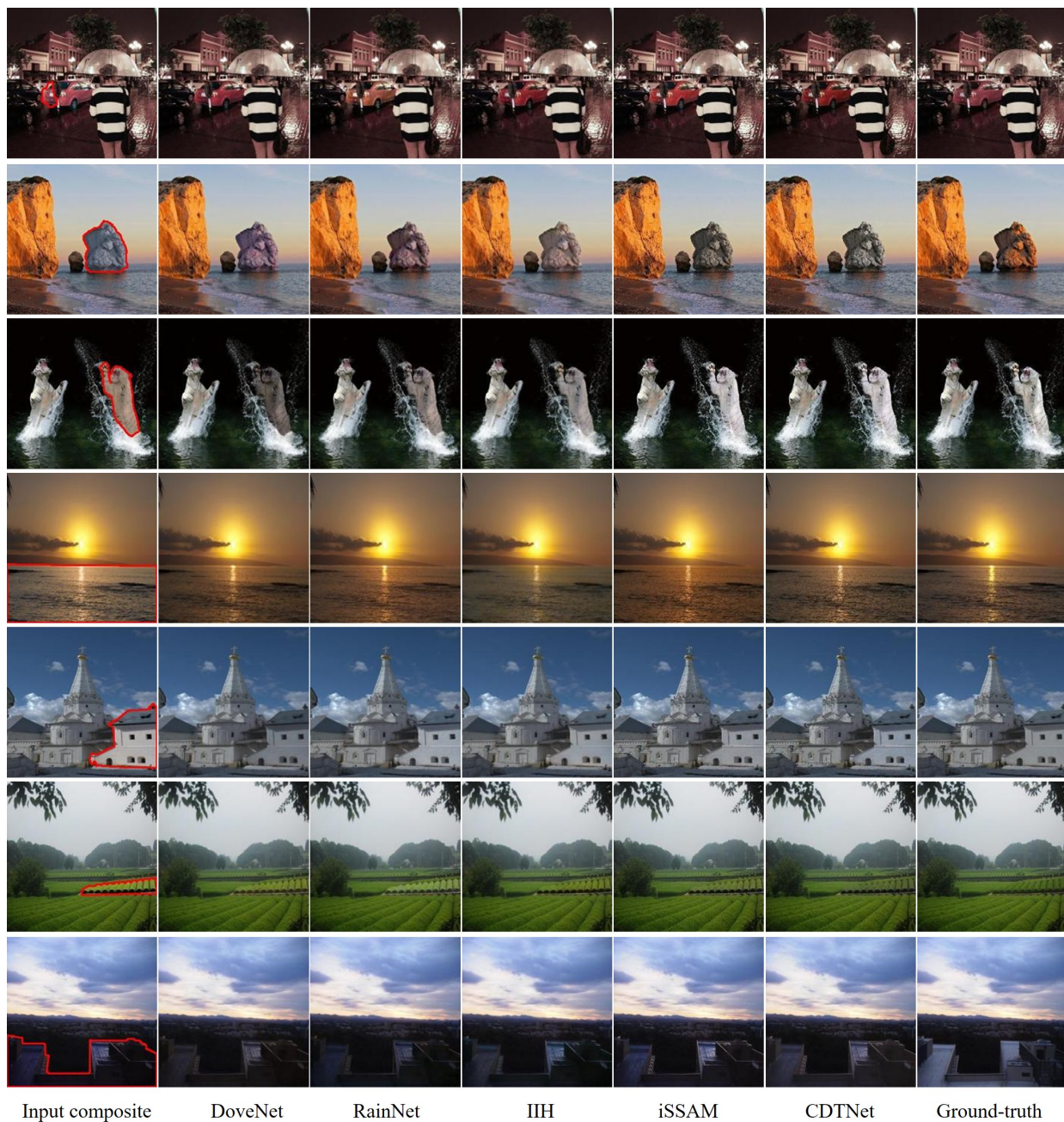


Fig. 12. The visualization results of different image harmonization methods on iHarmony4 dataset [17]. From left to right in each row, we show the input composite image, the harmonization results of DoveNet [17], RainNet [89], IIH [43], iSSAM [130], CDTNet [19]), and the ground-truth harmonized image.

additional Spatial-Separated Attention Module to deal with foreground and background feature maps separately. Hao et al. [47] employed self-attention [154] mechanism to propagate relevant information from background to foreground. By treating different capture conditions as different domains, Cong et al. [17] proposed a domain verification discriminator to pull close the foreground domain and background domain. Similarly, Cong et al. [18] formulated image harmonization as background-guided domain translation task, in which the domain code of background is directly used to guide the harmonization process. One byproduct of [18] is predicting the inharmony level of an image by comparing the domain codes

of foreground and background, so that we can selectively harmonize those apparently inharmonious composite images. Inspired by [18], Valanarasu et al. [147] proposed to extract style code from part of background.

In [89], they reframed image harmonization as a background-to-foreground style transfer problem and introduced region-aware adaptive instance normalization (AdaIn) to transfer visual style from the background to the foreground. A succeeding work [46] extended [89] by searching foreground-relevant background regions and transferring foreground-relevant style from background to foreground. They also extended the triplet loss in [18] to contrastive loss.

Analogous to [5] using Retinex theory, Guo et al. [43] also developed a model to disentangle a composite image into reflectance map and illumination map, in which the illumination map is harmonized by transferring lighting information from background to foreground. Another work [42] also adopted the similar decomposition network and explored integrating transformer block [148] into the network, which is further extended to [44]. Following the disentanglement technical route, Jiang et al. [59] proposed to disentangle an image into content representation and appearance representation. Then, the appearance representation of foreground is superseded by that of background to accomplish the goal of image harmonization.

Inspired by traditional image harmonization methods [168, 133] which applied color transformation to adjust the foreground appearance, Cong et al. [19] proposed to learn color transformation using deep learning for image harmonization. They combined color-to-color transformation and pixel-to-pixel transformation in a unified framework coherently. Several other works [167, 85, 119, 64, 41, 151] also proposed to predict various types of color transformations (*e.g.*, color filter, rendering curve, linear transformation) for efficient image harmonization.

Some recent works [108, 125, 13] concurred that dynamic kernels acting upon feature maps can boost the harmonization performance. Furthermore, [108, 125] pointed out the importance of global information in dynamic kernel prediction. Niu et al. [107] studied domain adaptive image harmonization by treating different datasets as different domains. Specifically, an automatic augmentation network was developed to enrich the illumination diversity of a target domain with limited data.

C. Variants of Image Harmonization Task

In this subsection, we discuss two variants of standard image harmonization task.

Blind image harmonization: Most image harmonization methods require the foreground mask as input, which means that the inharmonious region is known in advance. However, in real-world applications, we may not know the exact inharmonious region in advance. Image harmonization without foreground mask is called blind image harmonization. Cun and Pun [21] considered the problem of blind image harmonization. They proposed to predict the inharmonious region mask in the attention block, which deals with the foreground and background separately according to the predicted mask. Subsequently, some works [83, 84, 161, 160] focus on inharmonious region localization task, which aims to localize the inharmonious region in an image. Liang et al. [83] explored aggregating multi-scale contextual information and suppressing redundant information. The methods [84, 161] proposed to magnify the domain discrepancy between foreground and background using color mapping for ease of identifying the inharmonious region.

Painterly image harmonization: In standard image harmonization, both foreground and background are from realistic images. There exist certain application scenarios that the background is an artistic image while the foreground is

from a realistic image, in which case the standard image harmonization models may not work well. To overcome this problem, painterly image harmonization [101] has been studied to harmonize the realistic foreground according to the artistic background to obtain a uniformly stylized composite image. The relation between painterly image harmonization and standard image harmonization is like the relation between photorealistic style transfer and artistic style transfer. Painterly image harmonization is also referred to as cross-domain image composition [45, 98, 165]. The existing painterly image harmonization methods can be roughly categorized into optimization-based methods and feed-forward methods.

Optimization-based methods optimize the input image to minimize the style loss and content loss, which is very time-consuming. For example, Luan et al. [101] proposed to optimize the input image with two passes, in which the first pass aims at robust coarse harmonization and the second pass targets at high-quality refinement. Feed-forward methods send the input image through the model to output the harmonized result. For example, Peng et al. [112] applied adaptive instance normalization to match the means and variances between the feature map of composite image and that of artistic background. Cao et al. [10] performed painterly image harmonization in both frequency domain and spatial domain, considering that artistic paintings often have periodic textures and patterns which appear regularly. Lu et al. [97] introduced diffusion model to painterly image harmonization, which can significantly outperform GAN-based methods when the background has dense textures or abstract style.

D. Related Research Fields

Image harmonization is closely related to style transfer. Note that both artistic style transfer [36, 54, 111] and photorealistic style transfer [100, 82] belong to style transfer. Image harmonization is closer to photorealistic style transfer, which transfers the style of a reference photo to another input photo. There are two main differences between image harmonization and photorealistic style transfer. 1) Firstly, image harmonization adjusts the foreground appearance according to the background, which needs to take the foreground location into consideration due to the locality property. In contrast, photorealistic style transfer adjusts the appearance of a whole input image according to another whole reference image. 2) Secondly, the definition of “style” in photorealistic style transfer is unclear and coarsely depends on the employed style loss (*e.g.*, Gram matrix loss [36], AdaIn loss [54]). Differently, the goal of image harmonization is clearly adjusting the illumination statistics of foreground, so that the resultant foreground looks like the same object captured in the background illumination condition.

E. Datasets and Evaluation Metrics

A large amount of composite images can be easily obtained by pasting the foreground from one image on another background image, but it is not easy to obtain the ground-truth harmonized image for the composite image. Training deep learning models requires abundant pairs of composite images

and ground-truth harmonized images. Existing works have designed different schemes to construct image harmonization dataset. We categorize the existing schemes into three groups: forward adjustment, backward adjustment, and replacement. Note that some datasets are constructed based on real images while some other datasets are constructed using rendering techniques. We summarize the existing image harmonization datasets in Fig. 10. Moreover, we show one representative dataset from each group in Fig. 11.

Forward adjustment: Jiang et al. [59] released a small-scale *RealHM* dataset with 216 image pairs, which is constructed by manually harmonizing the composite image. However, manually adjusting the foreground according to the background to obtain the ground-truth is time-consuming, labor-intensive, and unreliable.

Backward adjustment: In contrast with manually adjusting the foreground of composite image to create harmonized image, some other works [146, 21, 17] adopted an inverse approach, *i.e.*, adjusting the foreground of real image to create synthetic composite image. Specifically, they treat a real image as harmonized image, segment a foreground region, and adjust this foreground region to be inconsistent with the background, yielding a synthetic composite image. Cong et al. [17] released the first large-scale image harmonization dataset *iHarmony4* with 73146 pairs of synthetic composite images and ground-truth real images. *iHarmony4* consists of four sub-datasets, in which three sub-datasets (HCOCO, HFlickr, HAdobe5k) are constructed using the aforementioned scheme. HCOCO (*resp.*, HFlickr) sub-dataset is built upon COCO [88] (*resp.*, crawled images from Flickr website), in which the foregrounds in real images are adjusted using traditional color transfer methods [117, 163, 31, 114]. HAdobe5k sub-dataset is generated based on MIT-Adobe FiveK dataset [8], in which the foregrounds in real images are manually edited. When using automatic color transfer for foreground adjustment (*e.g.*, HCOCO, HFlickr), a large number of pairs of synthetic composite images and real images can be easily obtained.

Replacement: A natural way to build image harmonization dataset is collecting a set of foreground images captured in different illumination conditions, followed by replacing one foreground with another counterpart. For example, Transient Attributes Database [70] contains 101 sets, in which each set has well-aligned images for the same scene captured in different conditions (*e.g.*, weather, time of the day, season). This dataset has been used to construct pairs in Hday2night sub-dataset in *iHarmony4* [17]. However, collecting the dataset like [70] calls for capturing the same scene with a fixed camera for a long time, which is hard to be realized in practice. To obtain the foregrounds in different capture conditions, Song et al. [131] proposed an interesting way to construct *GMS* Dataset. Specifically, they place the same physical model (3D foreground object) in different lighting conditions to capture different images and align the foregrounds in different images. Nevertheless, the collection cost is still very high and the diversity of foreground is restricted. In lieu of capturing images in the real world, an easy alternative is varying the illumination condition in a virtual environment. Cao et al. [9] constructed *RdHarmony* dataset by varying the lighting

condition of the same scene using 3D rendering techniques. Within a set of images with the same scene yet various lighting conditions, the composite images could be obtained by exchanging the foregrounds between two images. Similarly, Guo et al. [43] constructed *HVIDIT* dataset based on the rendered dataset [26]. However, the rendered images have large domain gap with real images, so the harmonization model trained on rendered images cannot be directly applied to real test images.

For quantitative evaluation, existing works adopt metrics including Mean Square Error (MSE), Peak Signal-to-Noise Ratio (PSNR), Structural SIMilarity index (SSIM) [122], Learned Perceptual Image Patch Similarity (LPIPS) [182] to calculate the distance between harmonized result and ground-truth. These metrics can also be calculated only within the foreground region. For qualitative evaluation, they conduct user study on real composite images by asking engaged users to select the most realistic images and calculate the metric (*e.g.*, B-T score [6]).

F. Experiments

Since *iHarmony4* [17], which includes HCOCO, HFlickr, HAdobe5k, and Hday2night, is the most commonly used dataset for image harmonization, we evaluate different methods on *iHarmony4* dataset. All methods are trained on the combination of training sets from four sub-datasets, and evaluated on the test set from each sub-dataset.

In Fig. 12, we show the harmonized results of different methods (DoveNet [17], RainNet [89], IIH [43], iSSAM [130], CDTNet [19]). We observe that some competitive methods can generally produce visually appealing results that are close to the ground-truth images. However, when the background illumination is very complex or the composite foreground and background have dramatically divergent illumination statistics, the existing methods are still struggling to harmonize the foreground to approach the ground-truth.

V. SHADOW GENERATION

In the previous section, image harmonization methods could adjust the foreground appearance to make it compatible with the background, but they ignore the fact that the inserted object may also have impact on the background (*e.g.*, reflection, shadow). For example, if background objects cast shadows on the ground but the inserted object does not have shadow, the composite image would look unrealistic. To address this issue, shadow generation task aims to generate plausible shadow for the foreground object according to background illumination information to make the composite image more realistic. Similar to Section IV, we divide the existing methods into rendering based methods and non-rendering based methods.

A. Rendering based Methods

The traditional methods [61, 62, 90, 86] usually use rendering techniques to generate shadow for the inserted foreground object, which needs to collect or estimate the scene geometry, foreground object geometry, and scene illumination. For example, [61] proposed to collect the rough geometry information

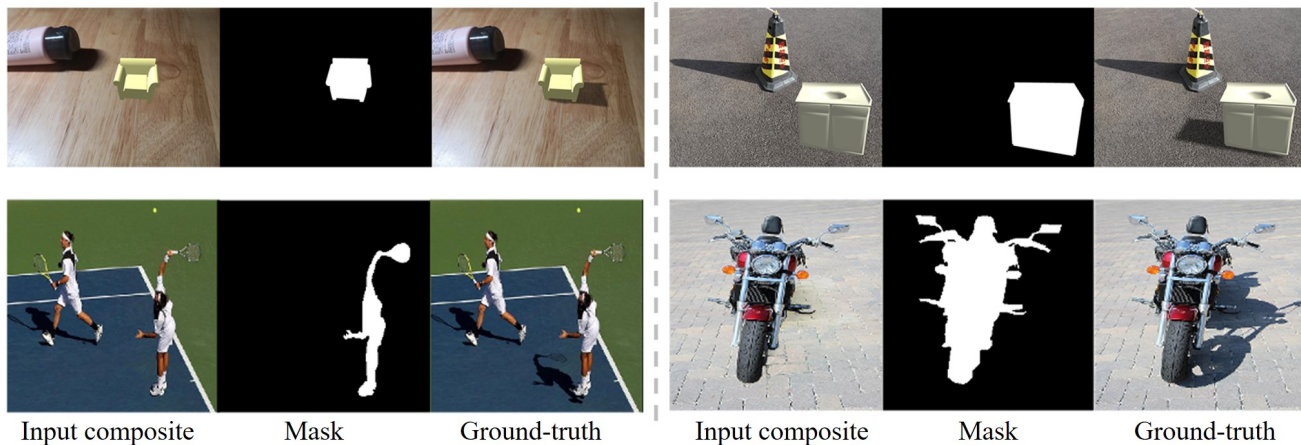


Fig. 13. In the first row, we show two examples from Shadow-AR dataset [91], which is constructed based on rendered images. In the second row, we show two examples from DESOBA dataset [50], which is constructed based on real images. From left to right in each example, we show the composite image without foreground shadow, the foreground mask, and the ground-truth image with foreground shadow.

and lighting information from users, based on which rendering techniques could be employed. However, it is very tedious and sometimes impossible to collect all the required information. In [62, 90, 86], they attempted to estimate the missing information (e.g., scene geometry, lighting information) automatically. With the recovered information, the local region to place the inserted 3D object is rendered with and without the inserted foreground object. The difference between these two rendered images reveals the impact of foreground object on the background, which is added to the input composite image to produce the target image with foreground shadow. Geometry estimation and lighting estimation based on a single image have been long studied, and many different technical approaches have been developed [90, 67]. More recently, some methods [86, 34, 177, 35, 49, 157] endeavored to estimate illumination condition and scene geometry based on a single image using deep learning models, which could achieve better performance than traditional estimation models. Some works [127, 128] proposed to forecast essential geometry information (e.g., pixel height) which cooperates with user-specified illumination to render realistic shadows.

Despite the remarkable progress they have achieved, it is still very challenging to accurately estimate the geometry and lighting information in complex real-world scenes. Erroneous estimation may mislead the rendering process and produce terrible results [184].

B. Non-rendering based Methods

Recently, some works treat shadow generation as an image-to-image translation task, and develop deep networks which translate input composite image without foreground shadow to the target image with foreground shadow. For instance, Zhan et al. [173] used an auto-encoder to predict the shadow mask with a pretrained illumination model [33, 16] to provide illumination information. The generated images are pushed towards real images with foreground shadows using adversarial learning.

Other methods [184, 55, 91, 50] utilized paired training data (paired images with and without foreground shadow) to generate better shadow images. ShadowGAN [184] employed standard conditional GAN with reconstruction loss, local adversarial loss, and global adversarial loss to generate shadow for the inserted 3D foreground objects. Inoue et al. [55] developed a multi-task framework with two decoders accounting for depth map prediction and ambient occlusion map prediction respectively. ARShadowGAN [91] proposed an attention-guided residual network. The network predicts two attention maps for background shadow and occluder respectively, which are concatenated with composite image and foreground object mask to produce a residual shadow image. SGRNet [50] designed a two-stage shadow generation network. In the first stage, foreground features and background features are interacted using cross-attention to predict a shadow mask. In the second stage, they predict shadow parameters which are used to darken the input composite image. Then, the darkened image is combined with the input composite image with shadow matte. Meng et al. [103] adopted a similar two-stage pipeline and proposed to generate the shadow region by fusing multiple underexposure images.

Some other shadow generation methods are not designed for our task, *i.e.*, generating shadow for the foreground object in a composite image, but they can be somehow adapted to our task. Mask-ShadowGAN [52] explored conducting shadow removal and shadow generation with unpaired data at the same time, which satisfies cyclic consistency. The shadow generation branch can be directly extended to generate foreground shadow. Sheng et al. [126] designed a shadow generation network to generate soft shadow for foreground object with user control. They first predict ambient occlusion map, which is jointly used with user-provided light map to produce soft shadow mask. When adapted to our task, an environment light map needs to be inferred from background before using their network.

The above methods can generate reasonable shadows for foreground objects in the composite images with simple scene

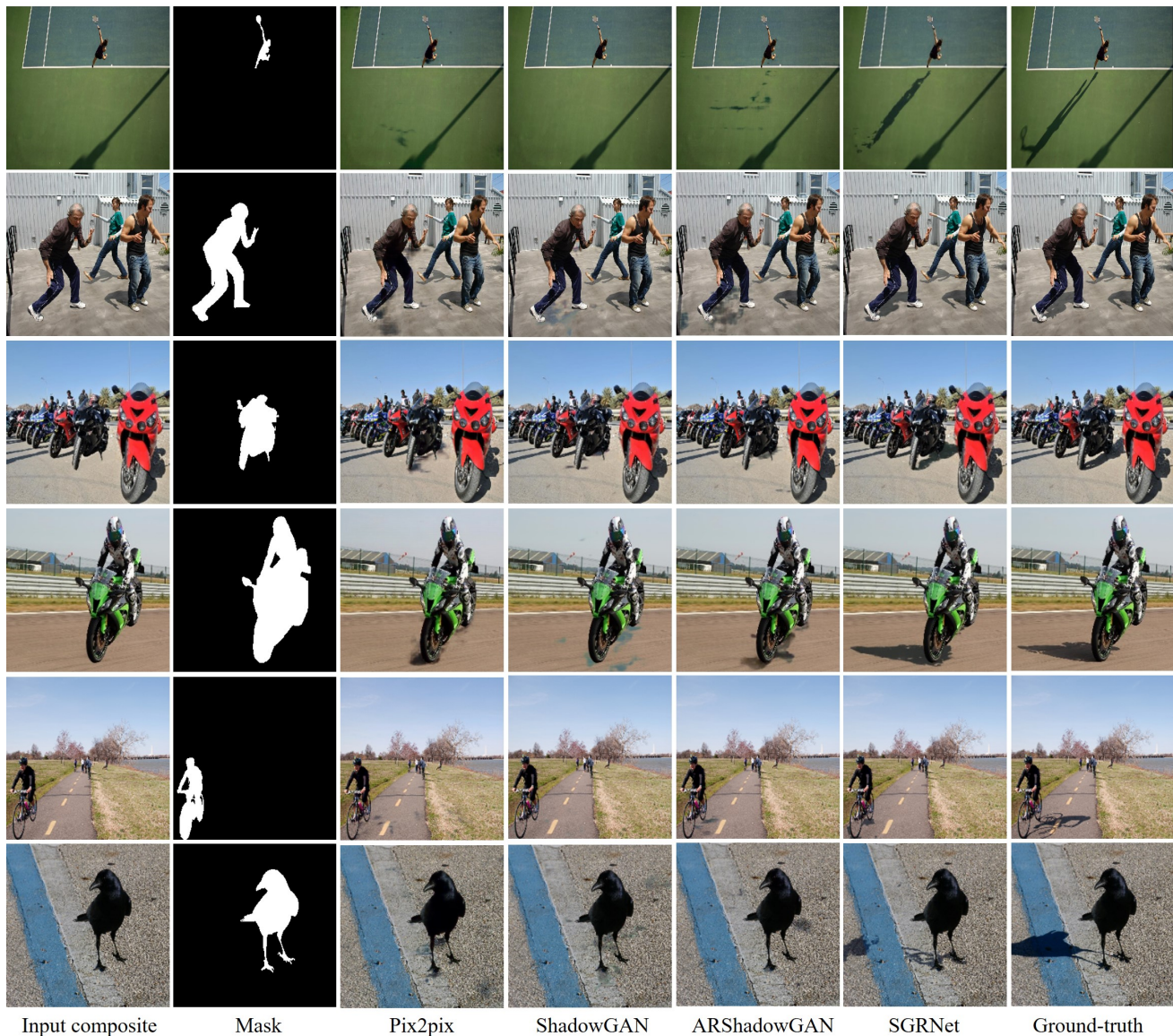


Fig. 14. The visualization results of different shadow generation methods on DESOBA dataset [50]. From left to right in each row, we show the input composite image, the composite foreground mask, the generated results of Pix2pix [56], ShadowGAN [184], ARShadowGAN [91], SGRNet [50], and the ground-truth shadow image.

and illumination condition, but often fail to generate reasonable shadows for the composite images with complex scene and illumination condition. Moreover, the generated shadows have roughly correct locations and shapes, but lack realistic contours and details matching the foreground objects.

C. Datasets and Evaluation Metrics

Similar to image harmonization in Section IV, composite images without foreground shadows can be easily obtained. Nonetheless, it is very difficult to obtain paired data, *i.e.*, a composite image without foreground shadow and a ground-truth image with foreground shadow, which are required by supervised deep learning methods on shadow generation [184, 91, 50]. Some works [184, 91] construct rendered datasets with paired data by inserting a virtual object into 3D scene and gen-

erating shadow for this object with rendering technique. ARShadowGAN [91] released a rendered dataset named *Shadow-AR* by inserting a foreground object into real background image and generating its corresponding shadow with rendering technique. Shadow-AR dataset contains 3,000 quintuples, in which each quintuple consists of a composite image without foreground shadow, its corresponding ground-truth image with foreground shadow, foreground object mask, background object mask, and background shadow mask. Shadow-AR dataset only uses 13 foreground objects from ShapeNet [11] and Stanford 3D scanning repository, so the diversity of dataset is very limited. Some examples in Shadow-AR dataset are exhibited in the first row in Fig. 13, in which we show the composite image without foreground shadow, foreground object mask, and ground-truth image with foreground shadow.

Similar to ARShadowGAN [91], ShadowGAN [184] also adopted rendering technique to construct a rendered dataset, which uses 9,265 foreground objects from ShapeNet [11] and 110 background textures (*e.g.*, woollen, stone, tablecloth) collected from Internet. Tao et al. [141] contributed a large-scale rendering dataset called RdSOBA, which has 788 3D foreground objects and nearly 280,000 object-shadow pairs. In particular, they place a group of 3D objects in the 3D scene, and get the images without or with object shadows using rendering techniques.

Although it is feasible to generate paired data using rendering technique, the rendered images have large domain gap with real images. When applying the model trained on rendered images to real images, the performances are usually significantly degraded. To overcome this drawback, Hong et al. [50] constructed paired data by manually removing the foreground shadows from real shadow images in SOBA dataset [152] to produce synthetic composite images without foreground shadows, leading to *DESOBA* dataset. This strategy to create synthetic composite image is similar to the backward adjustment for constructing image harmonization dataset (see Section IV). In particular, Hong et al. [50] first remove all shadows from a shadow image to create a shadow-free image. Then, one foreground shadow region in the shadow image is overlaid by the counterpart in its corresponding shadow-free image, yielding a synthetic composite image with one missing foreground shadow. *DESOBA* dataset contains 839 training images with totally 2,995 object-shadow pairs and 160 test images with totally 624 object-shadow pairs. Some examples in *DESOBA* dataset are exhibited in the second row in Fig. 13, in which we show the composite image without foreground shadow, foreground object mask, and ground-truth image with foreground shadow. As mentioned in [50], manual shadow removal is extremely expensive. With the rapid progress of shadow removal and image inpainting techniques, we can use automatic shadow removal to create large-scale datasets.

To evaluate the quality of generated composite images with foreground shadows, existing shadow generation works [173] without paired data adopt Frechet Inception Distance (FID) [48] and Manipulation Score (MS) [12] to measure the realism of generated shadow images. For the works [91, 50] with paired data, they adopt Structural SIMilarity index (SSIM) [122] and Root Mean Square Error (RMSE) [4] to measure the difference between generated image and ground-truth image. SSIM and RMSE can also be calculated only within the ground-truth foreground shadow region. Liu et al. [91] also use Balanced Error Rate (BER) [105] to evaluate the quality of predicted shadow mask based on ground-truth shadow mask.

D. Experiments

We compare existing shadow generation methods ShadowGAN [184], ARShadowGAN [91], and SGRNet [50] on the *DESOBA* dataset [50]. We also include classic paired image-to-image translation method Pix2pix [56] for comparison. We show the shadow images generated by different methods in Fig. 14. It can be seen that most methods are struggling

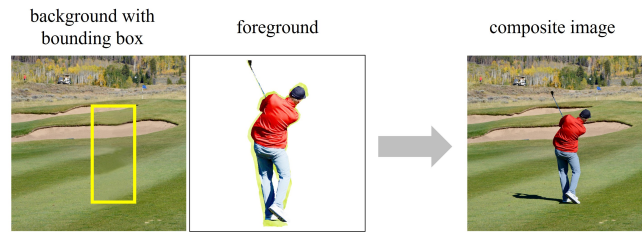


Fig. 15. Given a foreground image and a background image with bounding box indicating the foreground placement, generative image composition aims to produce a realistic composite image.

to produce reasonable shadow for the foreground object, or even produce no shadow at all, which implies that shadow generation for the inserted foreground object is a very tough task. Among the existing methods, SGRNet [50] achieves relatively compelling results, but the shapes of generated shadows are unrealistic and there is still plenty of room for improvement.

VI. GENERATIVE COMPOSITION

As the diffusion models [120] pretrained on large-scale dataset [123] become popular in various image generation and editing tasks, generative image composition has attracted growing research interest. In contrast with previous methods which perform one or multiple sub-tasks sequentially, generative image composition is a combinatorial task which performs multiple sub-tasks (*e.g.*, image blending, image harmonization, shadow generation) parallelly through one unified model. Given a foreground, a background, and a bounding box indicating the foreground placement, generative image composition targets at directly producing a realistic composite image with the foreground naturally and harmoniously merged into the background, as shown in Fig. 15.

A. Deep Learning Methods

The existing generative image composition methods can be divided into two groups. The first group of methods [169, 132, 15, 186] train a diffusion model on abundant pairs of foregrounds and backgrounds, so that it can be directly applied to a new pair of foreground and background at test time. In [169, 132], they construct massive training triplets of foregrounds, backgrounds, and ground-truth real images based on large-scale image datasets [69]. Then, they adapt conditional diffusion model to this task. In particular, the background image, bounding box mask, and noisy image are concatenated as input, while the foreground is injected into the network via cross-attention. Kulal et al. [68] adopted a similar approach, but focused on human generation. Chen et al. [15] proposed to enhance the foreground fidelity by using high-frequency information.

The second group of methods adapt a pretrained diffusion model to a subject by finetuning on a few reference images of this subject, inspired by [121]. For example, DreamEdit [79] proposed to finetune the diffusion model to associate a special token with one specific subject, and then perform iterative

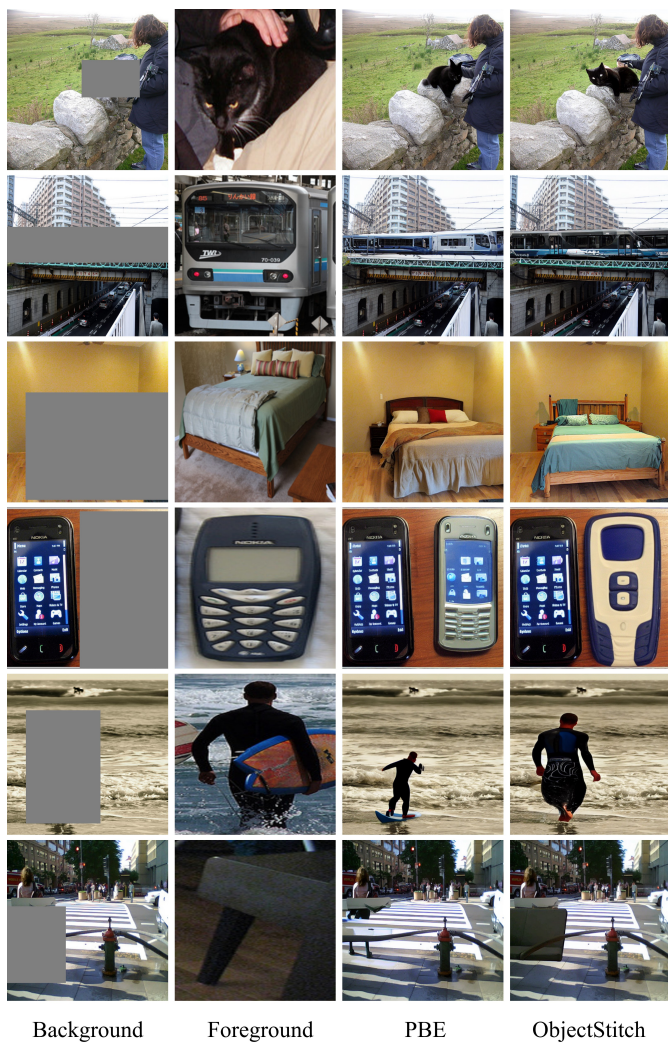


Fig. 16. The visualization results of PBE [169] and ObjectStitch [132] for generative image composition.

inpainting to combine foreground and background. This group of methods can leverage multiple reference images of a single subject, but they are very time-consuming due to finetuning the pretrained diffusion model for each subject.

Generative image composition methods perform multiple sub-tasks parallelly through a unified model, which is more concise than performing multiple sub-tasks sequentially. Nevertheless, the controllability is compromised in the meanwhile and undesirable changes (*e.g.*, unnecessary pose adjustment) could be made towards the foreground.

B. Datasets and Evaluation Metrics

Training diffusion model requires massive training triplets of foregrounds, backgrounds, and ground-truth real images. Previous works [169, 132] proposed to crop the foregrounds from real images and perturb the foregrounds (*e.g.*, color transfer, geometric transformation), so that we can have perturbed foreground, masked background, and ground-truth real image. Chen et al. [15] argued that such simple perturbation cannot simulate real-world viewpoint change, so they resorted

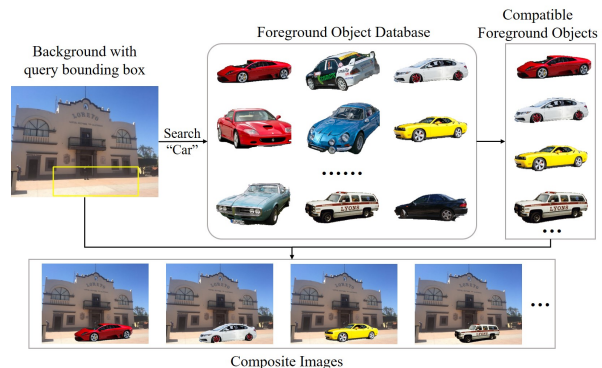


Fig. 17. Illustration of foreground object search. Given a background image with query bounding box (yellow), foreground object search aims to find compatible foreground objects of a specified category from a library, which is composited with the background to produce a realistic composite image.

to multi-view image datasets and video datasets to get more reasonably perturbed foregrounds.

In real-world application scenarios, there exist no ground-truth images for a pair of foreground and background, so we cannot calculate the distance between generated image and ground-truth image. Therefore, previous works [169, 132, 15, 186] used FID [48] to measure the discrepancy between generated images and real images, quality score [40] to evaluate the authenticity of each image, and CLIP score [116] to measure the similarity between generated foreground and reference foreground.

C. Experiments

We evaluate different methods [169, 132] on COCOEE test set provided by [169] and show the visualization results in Fig. 16. We can observe that they have the potential to produce high-quality composite images, in which the foregrounds are realistic and compatible with background. Even for the drastic viewpoint change (*e.g.*, row 2), they are capable of producing impressive results. However, in some challenging cases, the generated results may lose the details of foreground object (*e.g.*, row 3, row 4) or contain noticeable artifacts (*e.g.*, row 6). Additionally, they require manual specification of reasonable bounding box and cannot generate shadow that falls out of the bounding box, so object placement and shadow generation are actually not fully accomplished.

VII. FOREGROUND OBJECT SEARCH

The goal of foreground object search (FOS) is retrieving suitable foregrounds from a foreground library, which are compatible with the background in terms of illumination, geometry, and semantics. The FOS task is illustrated in Fig. 17. Finding compatible foregrounds can greatly alleviate the burden of creating realistic composite images, which is complementary with the other image composition techniques. FOS task can be divided into constrained or unconstrained according to whether specifying the foreground category.

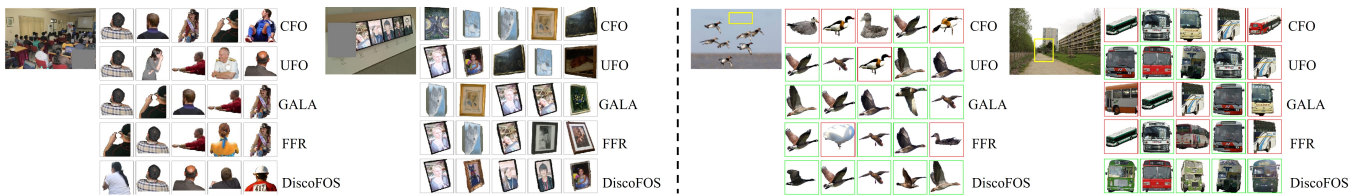


Fig. 18. The visualization results of different foreground object search methods CFO [187], UFO [188], GALA [191], FFR [162], DiscoFOS [175] on S-FOSD (left) and R-FOSD (right) datasets. On R-FOSD test set, green (*resp.*, red) box is used to indicate the foreground with compatible (*resp.*, incompatible) label.

A. Traditional Methods

Early works [72, 14] attempted to match each foreground with the background using hand-crafted features, but their performance is limited by the representation ability of hand-crafted features. Specifically, Lalonde et al. [72] estimated the object information (*e.g.*, size, orientation, lighting condition) and designed matching criteria to rank all the objects in the library. Chen et al. [14] exploited the contour consistency and content consistency between foreground and background based on hand-crafted features.

B. Deep Learning Methods

Recent work used deep learning features for foreground retrieval. For example, Tan et al. [135] utilized deep features to capture local context particularly for person compositing. Zhu et al. [190] trained a composite image discriminator to predict the realism of composites by compositing each foreground with the background. This method is effective by using the realism of composite image to measure the foreground-background compatibility, but computing the realism of all composite images is very expensive. More recent methods [187, 188, 191, 162, 75, 175] typically trained two encoders to extract foreground feature and background feature. Then, the foreground-background compatibility is measured by calculating the distance between foreground feature and background feature. They share the similar framework, despite the difference in data preparation, network structure, and loss design. Zhang et al. [175] observed that a composite image discriminator [190] can perform much better than two encoders, so they developed a teacher-student network which distills composite image feature from discriminator to the interaction output of foreground feature and background feature.

As introduced in Section I, the foreground and background in a composite image have multiple types of inconsistencies. The existing FOS works considered different sets of inconsistencies between background and foreground. For example, the methods [187, 188] considered the semantic consistency. The methods [75, 175] considered the geometry consistency and semantic consistency. Besides the geometry and semantic consistency, some other methods [162, 191] additionally considered style consistency [162] or lighting consistency [191].

C. Datasets and Evaluation Metrics

Early FOS works [187, 188, 162, 191] did not release their datasets. Zhang et al. [175] contributed two datasets: S-FOSD and R-FOSD, which contain synthetic composite

images and real composite images respectively. In S-FOSD dataset, Zhang et al. [175] segment one foreground object from a real image and fill its bounding box with image mean values to get the background. For each background image, the foreground object from the same image is deemed as ground-truth. In R-FOSD dataset, Zhang et al. [175] collect images from Internet as background images and draw a bounding box at the expected foreground location as query bounding box. R-FOSD dataset shares the same foregrounds with the test set of S-FOSD dataset. Zhang et al. [175] employ human annotators to label the compatibility of each pair of background and foreground. In comparison, S-FOSD dataset is low-cost and highly scalable, but has neither complete background nor ground-truth negative samples. R-FOSD dataset has complete background image with accurately annotated positive and negative foregrounds, yet is unscalable due to the high annotation cost.

On synthetic composite image dataset, Recall@k (R@k) is adopted as evaluation metric [187, 191, 175], which represents the percentage of background queries whose ground-truth foreground appears in top k retrievals. On real composite image dataset, mean Average Precision (mAP), mAP@20, and Precision@k (P@k) are adopted as evaluation metrics [188, 191, 175].

D. Experiments

We evaluate different methods on S-FOSD dataset and R-FOSD dataset [175]. Specifically, we train on S-FOSD training set, while testing on S-FOSD test set and R-FOSD test set. The retrieval results of CFO [187], UFO [188], GALA [191], FFR [162], and DiscoFOS [175] are shown in Fig. 18. The results show that DiscoFOS can retrieve more foregrounds that are compatible with the background.

VIII. CONCLUSION

In this paper, we have conducted a comprehensive survey on image composition, which involves a variety of techniques to produce a realistic composite image. We have introduced object placement, image blending, image harmonization, shadow generation, generative image composition, foreground object search in detail. In the future, we will extend this survey to more general composition in other fields such as video composition and 3D composition.

REFERENCES

- [1] Evline J Alappatt and Vince Paul. A survey on color transfer methods. *International Journal of Science, Engineering and Computer Technology*, 6(1):70, 2016.
- [2] Samaneh Azadi, Deepak Pathak, Sayna Ebrahimi, and Trevor Darrell. Compositional GAN: Learning image-conditional binary composition. *International Journal of Computer Vision*, 128(10):2570–2585, 2020.
- [3] Zhongyun Bao, Chengjiang Long, Gang Fu, Daquan Liu, Yuanzhen Li, Jiaming Wu, and Chunxia Xiao. Deep image-based illumination harmonization. In *CVPR*, 2022.
- [4] Jonathan T Barron and Jitendra Malik. Shape, illumination, and reflectance from shading. *IEEE Transactions on Pattern Analysis and Machine Intelligence*, 37(8):1670–1687, 2014.
- [5] Anand Bhattad and David A. Forsyth. Cut-and-paste neural rendering. *arXiv preprint arXiv:2010.05907*, 2020.
- [6] Ralph Allan Bradley and Milton E Terry. Rank analysis of incomplete block designs: I. the method of paired comparisons. *Biometrika*, 39(3/4):324–345, 1952.
- [7] Peter J Burt and Edward H Adelson. A multiresolution spline with application to image mosaics. *ACM Transactions on Graphics*, 2(4):217–236, 1983.
- [8] Vladimir Bychkovsky, Sylvain Paris, Eric Chan, and Frédo Durand. Learning photographic global tonal adjustment with a database of input / output image pairs. In *CVPR*, 2011.
- [9] Junyan Cao, Wenyan Cong, Li Niu, Jianfu Zhang, and Liqing Zhang. Deep image harmonization by bridging the reality gap. *BMVC*, 2022.
- [10] Junyan Cao, Yan Hong, and Li Niu. Painterly image harmonization in dual domains. In *AAAI*, 2023.
- [11] Angel X Chang, Thomas Funkhouser, Leonidas Guibas, Pat Hanrahan, Qixing Huang, Zimo Li, Silvio Savarese, Manolis Savva, Shuran Song, Hao Su, et al. ShapeNet: An information-rich 3D model repository. *arXiv preprint arXiv: 1512.03012*, 2015.
- [12] Bor-Chun Chen and Andrew Kae. Toward realistic image compositing with adversarial learning. In *CVPR*, 2019.
- [13] Haoxing Chen, Zhangxuan Gu, Yaohui Li, Jun Lan, Changhua Meng, Weiqiang Wang, and Huaxiong Li. Hierarchical dynamic image harmonization. In *ACM MM*, 2023.
- [14] Tao Chen, Ming-Ming Cheng, Ping Tan, Ariel Shamir, and Shimin Hu. Sketch2Photo: internet image montage. *ACM SIGGRAPH Asia*, 2009.
- [15] Xi Chen, Lianghua Huang, Yu Liu, Yujun Shen, Deli Zhao, and Hengshuang Zhao. Anydoor: Zero-shot object-level image customization. *arXiv preprint arXiv: 2307.09481*, 2023.
- [16] Dachuan Cheng, Jian Shi, Yanyun Chen, Xiaoming Deng, and Xiaopeng Zhang. Learning scene illumination by pairwise photos from rear and front mobile cameras. *Computer Graphics Forum*, 37(7):213–221, 2018.
- [17] Wenyan Cong, Jianfu Zhang, Li Niu, Liu Liu, Zhixin Ling, Weiyuan Li, and Liqing Zhang. DoveNet: Deep image harmonization via domain verification. In *CVPR*, 2020.
- [18] Wenyan Cong, Li Niu, Jianfu Zhang, Jing Liang, and Liqing Zhang. BargainNet: Background-guided domain translation for image harmonization. In *ICME*, 2021.
- [19] Wenyan Cong, Xinhao Tao, Li Niu, Jing Liang, Xuesong Gao, Qihao Sun, and Liqing Zhang. High-resolution image harmonization via collaborative dual transformations. In *CVPR*, 2022.
- [20] Marius Cordts, Mohamed Omran, Sebastian Ramos, Timo Rehfeld, Markus Enzweiler, Rodrigo Benenson, Uwe Franke, Stefan Roth, and Bernt Schiele. The cityscapes dataset for semantic urban scene understanding. In *CVPR*, 2016.
- [21] Xiaodong Cun and Chi-Man Pun. Improving the harmony of the composite image by spatial-separated attention module. *IEEE Transactions on Image Processing*, 29:4759–4771, 2020.
- [22] Yutong Dai, Brian Price, He Zhang, and Chunhua Shen. Boosting robustness of image matting with context assembling and strong data augmentation. In *CVPR*, 2022.
- [23] Nikita Dvornik, Julien Mairal, and Cordelia Schmid. Modeling visual context is key to augmenting object detection datasets. In *ECCV*, 2018.
- [24] Nikita Dvornik, Julien Mairal, and Cordelia Schmid. On the importance of visual context for data augmentation in scene understanding. *IEEE transactions on pattern analysis and machine intelligence*, 43(6):2014–2028, 2019.
- [25] Debidatta Dwibedi, Ishan Misra, and Martial Hebert. Cut, paste and learn: Surprisingly easy synthesis for instance detection. In *ICCV*, 2017.
- [26] Majed El Helou, Ruofan Zhou, Johan Barthas, and Sabine Süsstrunk. VIDIT: Virtual image dataset for illumination transfer. *arXiv preprint arXiv:2005.05460*, 2020.
- [27] Mark Everingham, Luc Van Gool, Christopher K. I. Williams, John M. Winn, and Andrew Zisserman. The pascal visual object classes (VOC) challenge. *International Journal of Computer Vision*, 88(2):303–338, 2010.
- [28] Haoshu Fang, Jianhua Sun, Runzhong Wang, Minghao Gou, Yonglu Li, and Cewu Lu. InstaBoost: Boosting instance segmentation via probability map guided copy-pasting. In *ICCV*, 2019.
- [29] Hasan Sheikh Faridul, Tania Pouli, Christel Chamaret, Jürgen Stauder, Alain Trémeau, Erik Reinhard, et al. A survey of color mapping and its applications. *Eurographics (State of the Art Reports)*, 3(2):1, 2014.
- [30] Raanan Fattal, Dani Lischinski, and Michael Werman. Gradient domain high dynamic range compression. In *ACM Siggraph Computer Graphics*, 2002.
- [31] Ulrich Fecker, Marcus Barkowsky, and André Kaup. Histogram-based prefiltering for luminance and chromi-

- nance compensation of multiview video. *IEEE Transactions on Circuits and Systems for Video Technology*, 18(9):1258–1267, 2008.
- [32] Yu Fu and Yuezhen Hu. A survey on image matting methods based on deep learning. *Frontiers in Economics and Management*, 3(3):497–502, 2022.
- [33] Marc-André Gardner, Kalyan Sunkavalli, Ersin Yumer, Xiaohui Shen, Emiliano Gambaretto, Christian Gagné, and Jean-François Lalonde. Learning to predict indoor illumination from a single image. *ACM Transactions on Graphics*, 36(6):1–14, 2017.
- [34] Marc-André Gardner, Yannick Hold-Geoffroy, Kalyan Sunkavalli, Christian Gagné, and Jean-François Lalonde. Deep parametric indoor lighting estimation. In *ICCV*, 2019.
- [35] Mathieu Garon, Kalyan Sunkavalli, Sunil Hadap, Nathan Carr, and Jean-François Lalonde. Fast spatially-varying indoor lighting estimation. In *CVPR*, 2019.
- [36] Leon A Gatys, Alexander S Ecker, and Matthias Bethge. A neural algorithm of artistic style. *arXiv preprint arXiv:1508.06576*, 2015.
- [37] Georgios Georgakis, Md. Alimoor Reza, Arsalan Mousavian, Phi-Hung Le, and Jana Kosecka. Multiview RGB-D dataset for object instance detection. In *3DV*, 2016.
- [38] Georgios Georgakis, Arsalan Mousavian, Alexander C. Berg, and Jana Kosecka. Synthesizing training data for object detection in indoor scenes. In *RSS XIII*, 2017.
- [39] Golnaz Ghiasi, Yin Cui, Aravind Srinivas, Rui Qian, Tsung-Yi Lin, Ekin D. Cubuk, Quoc V. Le, and Barret Zoph. Simple copy-paste is a strong data augmentation method for instance segmentation. *arXiv preprint arXiv:2012.07177*, 2020.
- [40] Shuyang Gu, Jianmin Bao, Dong Chen, and Fang Wen. Giga: Generated image quality assessment. In *ECCV*, 2020.
- [41] Julian Jorge Andrade Guerreiro, Mitsuru Nakazawa, and Björn Stenger. PCT-Net: Full resolution image harmonization using pixel-wise color transformations. In *CVPR*, 2023.
- [42] Zonghui Guo, Dongsheng Guo, Haiyong Zheng, Zhaorui Gu, Bing Zheng, and Junyu Dong. Image harmonization with transformer. In *ICCV*, 2021.
- [43] Zonghui Guo, Haiyong Zheng, Yufeng Jiang, Zhaorui Gu, and Bing Zheng. Intrinsic image harmonization. In *CVPR*, 2021.
- [44] Zonghui Guo, Zhaorui Gu, Bing Zheng, Junyu Dong, and Haiyong Zheng. Transformer for image harmonization and beyond. *IEEE Transactions on Pattern Analysis and Machine Intelligence*, 2022.
- [45] Roy Hachnochi, Mingrui Zhao, Nadav Orzech, Rinon Gal, Ali Mahdavi-Amiri, Daniel Cohen-Or, and Amit Haim Bermano. Cross-domain compositing with pretrained diffusion models. *arXiv preprint arXiv:2302.10167*, 2023.
- [46] Yucheng Hang, Bin Xia, Wenming Yang, and Qingmin Liao. SCS-Co: Self-consistent style contrastive learning for image harmonization. In *CVPR*, 2022.
- [47] Guoqing Hao, Satoshi Iizuka, and Kazuhiro Fukui. Image harmonization with attention-based deep feature modulation. In *BMVC*, 2020.
- [48] Martin Heusel, Hubert Ramsauer, Thomas Unterthiner, Bernhard Nessler, and Sepp Hochreiter. GANs trained by a two time-scale update rule converge to a local nash equilibrium. In *NeurIPS*, 2017.
- [49] Yannick Hold-Geoffroy, Akshaya Athawale, and Jean-François Lalonde. Deep sky modeling for single image outdoor lighting estimation. In *CVPR*, 2019.
- [50] Yan Hong, Li Niu, Jianfu Zhang, and Liqing Zhang. Shadow generation for composite image in real-world scenes. *AAAI*, 2022.
- [51] Qibin Hou, Ming-Ming Cheng, Xiaowei Hu, Ali Borji, Zhuowen Tu, and Philip HS Torr. Deeply supervised salient object detection with short connections. In *CVPR*, 2017.
- [52] Xiaowei Hu, Yitong Jiang, Chi-Wing Fu, and Pheng-Ann Heng. Mask-ShadowGAN: Learning to remove shadows from unpaired data. In *ICCV*, 2019.
- [53] Zhongyun Hu, Ntumba Elie Nsambi, Xue Wang, and Qing Wang. NeSF: Neural shading field for image harmonization. *arXiv preprint arXiv:2112.01314*, 2021.
- [54] Xun Huang and Serge Belongie. Arbitrary style transfer in real-time with adaptive instance normalization. In *ICCV*, 2017.
- [55] Naoto Inoue, Daichi Ito, Yannick Hold-Geoffroy, Long Mai, Brian Price, and Toshihiko Yamasaki. RGB2ao: Ambient occlusion generation from RGB images. In *Computer Graphics Forum*, volume 39, pages 451–462, 2020.
- [56] Phillip Isola, Jun-Yan Zhu, Tinghui Zhou, and Alexei A Efros. Image-to-image translation with conditional adversarial networks. In *CVPR*, 2017.
- [57] Max Jaderberg, Karen Simonyan, Andrew Zisserman, and Koray Kavukcuoglu. Spatial transformer networks. In *NeurIPS*, 2015.
- [58] Jiaya Jia, Jian Sun, Chi-Keung Tang, and Heung-Yeung Shum. Drag-and-drop pasting. *ACM Transactions on graphics*, 25(3):631–637, 2006.
- [59] Yifan Jiang, He Zhang, Jianming Zhang, Yilin Wang, Zhe Lin, Kalyan Sunkavalli, Simon Chen, Sohrab Amirghodsi, Sarah Kong, and Zhangyang Wang. Ssh: A self-supervised framework for image harmonization. In *ICCV*, 2021.
- [60] Zhengxia Zou Keyan Chen Zhenwei Shi Jianqi Chen, Yilan Zhang. Dense pixel-to-pixel harmonization via continuous image representation. *arXiv preprint arXiv:2303.01681*, 2023.
- [61] Kevin Karsch, Varsha Hedau, David Forsyth, and Derek Hoiem. Rendering synthetic objects into legacy photographs. *ACM Transactions on Graphics*, 30(6):1–12, 2011.
- [62] Kevin Karsch, Kalyan Sunkavalli, Sunil Hadap, Nathan Carr, Hailin Jin, Rafael Fonte, Michael Sittig, and David Forsyth. Automatic scene inference for 3d object compositing. *ACM Transactions on Graphics*, 33(3):1–15, 2014.

- [63] Michael Kazhdan and Hugues Hoppe. Streaming multi-grid for gradient-domain operations on large images. *ACM Transactions on graphics*, 27(3):1–10, 2008.
- [64] Zhanghan Ke, Chunyi Sun, Lei Zhu, Ke Xu, and Rynson W.H. Lau. Harmonizer: Learning to perform white-box image and video harmonization. In *ECCV*, 2022.
- [65] Kotaro Kikuchi, Kota Yamaguchi, Edgar Simo-Serra, and Tetsunori Kobayashi. Regularized adversarial training for single-shot virtual try-on. In *ICCV Workshop*, 2019.
- [66] Ron Kimmel, Michael Elad, Doron Shaked, Renato Keshet, and Irwin Sobel. A variational framework for retinex. *International Journal of computer vision*, 52(1):7–23, 2003.
- [67] Joel Kronander, Francesco Banterle, Andrew Gardner, Ehsan Miandji, and Jonas Unger. Photorealistic rendering of mixed reality scenes. In *Computer Graphics Forum*, volume 34, pages 643–665, 2015.
- [68] Sumith Kulal, Tim Brooks, Alex Aiken, Jiajun Wu, Jimei Yang, Jingwan Lu, Alexei A. Efros, and Krishna Kumar Singh. Putting people in their place: Affordance-aware human insertion into scenes. In *CVPR*, 2023.
- [69] Alina Kuznetsova, Hassan Rom, Neil Gordon Alldrin, Jasper R. R. Uijlings, Ivan Krasin, Jordi Pont-Tuset, Shahab Kamali, Stefan Popov, Matteo Mallocci, Alexander Kolesnikov, Tom Duerig, and Vittorio Ferrari. The open images dataset v4. *International Journal of Computer Vision*, 128:1956–1981, 2020.
- [70] Pierre-Yves Laffont, Zhile Ren, Xiaofeng Tao, Chao Qian, and James Hays. Transient attributes for high-level understanding and editing of outdoor scenes. *ACM Transactions on graphics*, 33(4):1–11, 2014.
- [71] Jean-François Lalonde and Alexei A. Efros. Using color compatibility for assessing image realism. In *ICCV*, 2007.
- [72] Jean-François Lalonde, Derek Hoiem, Alexei A. Efros, Carsten Rother, John M. Winn, and Antonio Criminisi. Photo clip art. *ACM SIGGRAPH*, 2007.
- [73] Donghoon Lee, Sifei Liu, Jinwei Gu, Ming-Yu Liu, Ming-Hsuan Yang, and Jan Kautz. Context-aware synthesis and placement of object instances. In *NeurIPS*, 2018.
- [74] Anat Levin, Assaf Zomet, Shmuel Peleg, and Yair Weiss. Seamless image stitching in the gradient domain. In *ECCV*, 2004.
- [75] Boren Li, Po-Yu Zhuang, Jian Gu, Mingyang Li, and Ping Tan. Interpretable foreground object search as knowledge distillation. In *ECCV*, 2020.
- [76] Jizhizi Li, Sihan Ma, Jing Zhang, and Dacheng Tao. Privacy-preserving portrait matting. In *ACM MM*, 2021.
- [77] Jizhizi Li, Jing Zhang, and Dacheng Tao. Deep automatic natural image matting. *IJCAI*, 2021.
- [78] Jizhizi Li, Jing Zhang, Stephen J Maybank, and Dacheng Tao. Bridging composite and real: towards end-to-end deep image matting. *International Journal of Computer Vision*, 130(2):246–266, 2022.
- [79] Tianle Li, Max Ku, Cong Wei, and Wenhua Chen. Dreamedit: Subject-driven image editing. *arXiv preprint arXiv: 2306.12624*, 2023.
- [80] Xiang Li, Guowei Teng, Ping An, Haiyan Yao, and Yilei Chen. Advertisement logo compositing via adversarial geometric consistency pursuit. In *VCIP*, 2019.
- [81] Xiang Li, Guowei Teng, Ping An, and Hai-Yan Yao. Image synthesis via adversarial geometric consistency pursuit. *Signal Processing: Image Communication*, 99: 116489, 2021.
- [82] Yijun Li, Ming-Yu Liu, Xueting Li, Ming-Hsuan Yang, and Jan Kautz. A closed-form solution to photorealistic image stylization. In *ECCV*, 2018.
- [83] Jing Liang, Li Niu, and Liqing Zhang. Inharmonious region localization. In *ICME*, 2021.
- [84] Jing Liang, Li Niu, Penghao Wu, Fengjun Guo, and Teng Long. Inharmonious region localization by magnifying domain discrepancy. In *AAAI*, 2022.
- [85] Jingtang Liang, Xiaodong Cun, and Chi-Man Pun. Spatial-separated curve rendering network for efficient and high-resolution image harmonization. *ECCV*, 2022.
- [86] Bin Liao, Yao Zhu, Chao Liang, Fei Luo, and Chunxia Xiao. Illumination animating and editing in a single picture using scene structure estimation. *Computers & Graphics*, 82:53–64, 2019.
- [87] Chen-Hsuan Lin, Ersin Yumer, Oliver Wang, Eli Shechtman, and Simon Lucey. ST-GAN: spatial transformer generative adversarial networks for image compositing. In *CVPR*, 2018.
- [88] Tsung-Yi Lin, Michael Maire, Serge J. Belongie, James Hays, Pietro Perona, Deva Ramanan, Piotr Dollár, and C. Lawrence Zitnick. Microsoft COCO: common objects in context. In *ECCV*, 2014.
- [89] Jun Ling, Han Xue, Li Song, Rong Xie, and Xiao Gu. Region-aware adaptive instance normalization for image harmonization. In *CVPR*, 2021.
- [90] Bin Liu, Kun Xu, and Ralph R Martin. Static scene illumination estimation from videos with applications. *Journal of Computer Science and Technology*, 32(3): 430–442, 2017.
- [91] Daquan Liu, Chengjiang Long, Hongpan Zhang, Hanning Yu, Xinzhi Dong, and Chunxia Xiao. ARshadow-Gan: Shadow generative adversarial network for augmented reality in single light scenes. In *CVPR*, 2020.
- [92] Guilin Liu, Fitsum A Reda, Kevin J Shih, Ting-Chun Wang, Andrew Tao, and Bryan Catanzaro. Image inpainting for irregular holes using partial convolutions. In *ECCV*, 2018.
- [93] Liu Liu, Bo Zhang, Jiangtong Li, Li Niu, Qingyang Liu, and Liqing Zhang. OPA: Object placement assessment dataset. *arXiv preprint arXiv:2107.01889*, 2021.
- [94] Qinglin Liu, Haozhe Xie, Shengping Zhang, Bineng Zhong, and Rongrong Ji. Long-range feature propagating for natural image matting. In *ACM MM*, 2021.
- [95] Sheng Liu, Cong Phuoc Huynh, Cong Chen, Maxim Arap, and Raffay Hamid. Lemart: Label-efficient masked region transform for image harmonization. In *CVPR*, 2023.
- [96] Yuhao Liu, Jiake Xie, Xiao Shi, Yu Qiao, Yujie Huang,

- Yong Tang, and Xin Yang. Tripartite information mining and integration for image matting. In *ICCV*, 2021.
- [97] Lingxiao Lu, Jiangtong Li, Junyan Cao, Li Niu, and Liqing Zhang. Painterly image harmonization using diffusion model. In *ACM MM*, 2023.
- [98] Shilin Lu, Yanzhu Liu, and Adams Wai-Kin Kong. Tf-Icon: Diffusion-based training-free cross-domain image composition. *arXiv preprint arXiv:2307.12493*, 2023.
- [99] Xin Lu, Zhe Lin, Hailin Jin, Jianchao Yang, and James Z Wang. A structure-preserving and illumination-consistent cycle framework for image harmonization. *IEEE Transactions on Multimedia*, 2022.
- [100] Fujun Luan, Sylvain Paris, Eli Shechtman, and Kavita Bala. Deep photo style transfer. In *CVPR*, 2017.
- [101] Fujun Luan, Sylvain Paris, Eli Shechtman, and Kavita Bala. Deep painterly harmonization. In *Computer graphics forum*, volume 37, pages 95–106, 2018.
- [102] Shengjie Ma, Qian Shen, Qiming Hou, Zhong Ren, and Kun Zhou. Neural compositing for real-time augmented reality rendering in low-frequency lighting environments. *Science China Information Sciences*, 64(2):1–15, 2021.
- [103] Quanling Meng, Shengping Zhang, Zonglin Li, Chenyang Wang, Weigang Zhang, and Qingming Huang. Automatic shadow generation via exposure fusion. *IEEE Transactions on Multimedia*, 2023.
- [104] Shervin Minaee, Yuri Y Boykov, Fatih Porikli, Antonio J Plaza, Nasser Kehtarnavaz, and Demetri Terzopoulos. Image segmentation using deep learning: A survey. *IEEE Transactions on Pattern Analysis and Machine Intelligence*, 2021.
- [105] Vu Nguyen, Tomas F Yago Vicente, Maozheng Zhao, Minh Hoai, and Dimitris Samaras. Shadow detection with conditional generative adversarial networks. In *ICCV*, 2017.
- [106] Li Niu, Qingyang Liu, Zhenchen Liu, and Jiangtong Li. Fast object placement assessment. *arXiv preprint arXiv:2205.14280*, 2022.
- [107] Li Niu, Junyan Cao, Wenyan Cong, and Liqing Zhang. Deep image harmonization with learnable augmentation. In *ICCV*, 2023.
- [108] Li Niu, Linfeng Tan, Xinhao Tao, Junyan Cao, Fengjun Guo, Teng Long, and Liqing Zhang. Deep image harmonization with globally guided feature transformation and relation distillation. In *ICCV*, 2023.
- [109] Xi Ouyang, Yu Cheng, Yifan Jiang, Chun-Liang Li, and Pan Zhou. Pedestrian-synthesis-gan: Generating pedestrian data in real scene and beyond. *arXiv preprint arXiv:1804.02047*, 2018.
- [110] Rohit Kumar Pandey, Sergio Orts Escolano, Chloe LeGendre, Christian Haene, Sofien Bouaziz, Christoph Rhemann, Paul Debevec, and Sean Fanello. Total relighting: Learning to relight portraits for background replacement. In *SIGGRAPH*, 2021.
- [111] Dae Young Park and Kwang Hee Lee. Arbitrary style transfer with style-attentional networks. In *CVPR*, 2019.
- [112] Hwai-Jin Peng, Chia-Ming Wang, and Yu-Chiang Frank Wang. Element-embedded style transfer networks for style harmonization. In *BMVC*, 2019.
- [113] Patrick Pérez, Michel Gangnet, and Andrew Blake. Poisson image editing. In *ACM SIGGRAPH*. 2003.
- [114] François Pitié, Anil C Kokaram, and Rozenn Dahyot. Automated colour grading using colour distribution transfer. *Computer Vision and Image Understanding*, 107(1-2):123–137, 2007.
- [115] Thomas Porter and Tom Duff. Compositing digital images. In *ACM Siggraph Computer Graphics*, 1984.
- [116] Alec Radford, Jong Wook Kim, Chris Hallacy, Aditya Ramesh, Gabriel Goh, Sandhini Agarwal, Girish Sastry, Amanda Askell, Pamela Mishkin, Jack Clark, Gretchen Krueger, and Ilya Sutskever. Learning transferable visual models from natural language supervision. In *ICML*, 2021.
- [117] Erik Reinhard, Michael Ashikhmin, Bruce Gooch, and Peter Shirley. Color transfer between images. *IEEE Computer Graphics and Applications*, 21(5):34–41, 2001.
- [118] Tal Remez, Jonathan Huang, and Matthew Brown. Learning to segment via cut-and-paste. In *ECCV*, 2018.
- [119] Xuqian Ren and Yifan Liu. Semantic-guided multi-mask image harmonization. In *ECCV*, 2022.
- [120] Robin Rombach, Andreas Blattmann, Dominik Lorenz, Patrick Esser, and Björn Ommer. High-resolution image synthesis with latent diffusion models. In *CVPR*, 2022.
- [121] Nataniel Ruiz, Yuanzhen Li, Varun Jampani, Yael Pritch, Michael Rubinstein, and Kfir Aberman. Dreambooth: Fine tuning text-to-image diffusion models for subject-driven generation. In *CVPR*, 2023.
- [122] Tiago A Schieber, Laura Carpi, Albert Díaz-Guilera, Panos M Pardalos, Cristina Masoller, and Martín G Ravetti. Quantification of network structural dissimilarities. *Nature Communications*, 8(1):1–10, 2017.
- [123] Christoph Schuhmann, Richard Vencu, Romain Beaumont, Robert Kaczmarczyk, Clayton Mullis, Aarush Katta, Theo Coombes, Jenia Jitsev, and Aran Komatsuzaki. LAION-400M: Open dataset of clip-filtered 400 million image-text pairs. *arXiv preprint arXiv:2111.02114*, 2021.
- [124] Xiaoyong Shen, Aaron Hertzmann, Jiaya Jia, Sylvain Paris, Brian Price, Eli Shechtman, and Ian Sachs. Automatic portrait segmentation for image stylization. In *Computer Graphics Forum*, volume 35, pages 93–102, 2016.
- [125] Xintian Shen, Jiangning Zhang, Jun Chen, Shipeng Bai, Yue Han, Yabiao Wang, Chengjie Wang, and Yong Liu. Learning global-aware kernel for image harmonization. In *ICCV*, 2023.
- [126] Yichen Sheng, Jianming Zhang, and Bedrich Benes. SSN: Soft shadow network for image compositing. In *CVPR*, 2021.
- [127] Yichen Sheng, Yifan Liu, Jianming Zhang, Wei Yin, A. Cengiz Oztireli, He Zhang, Zhe Lin, Eli Shechtman, and Bedrich Benes. Controllable shadow generation using pixel height maps. In *ECCV*, 2022.
- [128] Yichen Sheng, Jianming Zhang, Julie Philip, Yannick

- Hold-Geoffroy, Xin Sun, He Zhang, Lu Ling, and Bedrich Benes. Pixht-lab: Pixel height based light effect generation for image compositing. In *CVPR*, 2023.
- [129] Zhixin Shu, Sunil Hadap, Eli Shechtman, Kalyan Sunkavalli, Sylvain Paris, and Dimitris Samaras. Portrait lighting transfer using a mass transport approach. *ACM Transactions on Graphics*, 36(4):1, 2017.
- [130] Konstantin Sofiiuk, Polina Popenova, and Anton Konushin. Foreground-aware semantic representations for image harmonization. In *WACV*, 2021.
- [131] Shuangbing Song, Fan Zhong, Xueying Qin, and Changhe Tu. Illumination harmonization with gray mean scale. In *Computer Graphics International Conference*, 2020.
- [132] Yizhi Song, Zhifei Zhang, Zhe Lin, Scott Cohen, Brian Price, Jianming Zhang, Soo Ye Kim, and Daniel Aliaga. Objectstitch: Generative object compositing. In *CVPR*, 2023.
- [133] Kalyan Sunkavalli, Micah K. Johnson, Wojciech Matusik, and Hanspeter Pfister. Multi-scale image harmonization. *ACM Transactions on Graphics*, 29(4):125:1–125:10, 2010.
- [134] Richard Szeliski, Matthew Uyttendaele, and Drew Steedly. Fast poisson blending using multi-splines. In *ICCP*, 2011.
- [135] Fuwen Tan, Crispin Bernier, Benjamin Cohen, Vicente Ordonez, and Connelly Barnes. Where and who? automatic semantic-aware person composition. In *WACV*, 2018.
- [136] Linfeng Tan, Jiangtong Li, Li Niu, and Liqing Zhang. Deep image harmonization in dual color spaces. In *ACM MM*, 2023.
- [137] Xuehan Tan, Panpan Xu, Shihui Guo, and Wencheng Wang. Image composition of partially occluded objects. In *Computer Graphics Forum*, volume 38, pages 641–650, 2019.
- [138] Masayuki Tanaka, Ryo Kamio, and Masatoshi Okutomi. Seamless image cloning by a closed form solution of a modified poisson problem. In *SIGGRAPH Asia 2012 Posters*. 2012.
- [139] Litian Tao, Lu Yuan, and Jian Sun. Skyfinder: attribute-based sky image search. *ACM transactions on graphics*, 28(3):1–5, 2009.
- [140] Michael W Tao, Micah K Johnson, and Sylvain Paris. Error-tolerant image compositing. In *ECCV*, 2010.
- [141] Xinhao Tao, Junyan Cao, and Li Niu. RdSOBA: Rendered shadow-object association dataset. *arXiv preprint arXiv: 2306.17358*, 2023.
- [142] Ayush Tewari, Tae-Hyun Oh, Tim Weyrich, Bernd Bickel, Hans-Peter Seidel, Hanspeter Pfister, Wojciech Matusik, Mohamed Elgharib, Christian Theobalt, et al. Monocular reconstruction of neural face reflectance fields. In *CVPR*, 2021.
- [143] Chunwei Tian, Lunke Fei, Wenxian Zheng, Yong Xu, Wangmeng Zuo, and Chia-Wen Lin. Deep learning on image denoising: An overview. *Neural Networks*, 131: 251–275, 2020.
- [144] Shashank Tripathi, Siddhartha Chandra, Amit Agrawal, Ambrish Tyagi, James M. Rehg, and Vivesh Chari. Learning to generate synthetic data via compositing. In *CVPR*, 2019.
- [145] Yi-Hsuan Tsai, Xiaohui Shen, Zhe Lin, Kalyan Sunkavalli, and Ming-Hsuan Yang. Sky is not the limit: semantic-aware sky replacement. *ACM Trans. Graph.*, 35(4):149–1, 2016.
- [146] Yi-Hsuan Tsai, Xiaohui Shen, Zhe Lin, Kalyan Sunkavalli, Xin Lu, and Ming-Hsuan Yang. Deep image harmonization. In *CVPR*, 2017.
- [147] Jeya Maria Jose Valanarasu, He Zhang, Jianming Zhang, Yilin Wang, Zhe Lin, Jose Echevarria, Yinglan Ma, Zijun Wei, Kalyan Sunkavalli, and Vishal M. Patel. Interactive portrait harmonization. In *ICLR*, 2023.
- [148] Ashish Vaswani, Noam Shazeer, Niki Parmar, Jakob Uszkoreit, Llion Jones, Aidan N Gomez, Łukasz Kaiser, and Illia Polosukhin. Attention is all you need. *NIPS*, 30, 2017.
- [149] Anna Volokitina, Igor Susmelj, Eirikur Agustsson, Luc Van Gool, and Radu Timofte. Efficiently detecting plausible locations for object placement using masked convolutions. In *ECCV workshop*, 2020.
- [150] Hao Wang, Qilong Wang, Fan Yang, Weiqi Zhang, and Wangmeng Zuo. Data augmentation for object detection via progressive and selective instance-switching. *arXiv preprint arXiv:1906.00358*, 2019.
- [151] Ke Wang, Michaël Gharbi, He Zhang, Zhihao Xia, and Eli Shechtman. Semi-supervised parametric real-world image harmonization. In *CVPR*, 2023.
- [152] Tianyu Wang, Xiaowei Hu, Qiong Wang, Pheng-Ann Heng, and Chi-Wing Fu. Instance shadow detection. In *CVPR*, 2020.
- [153] Xiaolong Wang, Rohit Girdhar, and Abhinav Gupta. Binge watching: Scaling affordance learning from sitcoms. In *CVPR*, 2017.
- [154] Xiaolong Wang, Ross Girshick, Abhinav Gupta, and Kaiming He. Non-local neural networks. In *CVPR*, 2018.
- [155] Zhibo Wang, Xin Yu, Ming Lu, Quan Wang, Chen Qian, and Feng Xu. Single image portrait relighting via explicit multiple reflectance channel modeling. *ACM Transactions on Graphics*, 39(6):1–13, 2020.
- [156] Zhihao Wang, Jian Chen, and Steven C. H. Hoi. Deep learning for image super-resolution: A survey. *IEEE Trans. Pattern Anal. Mach. Intell.*, 43(10):3365–3387, 2021.
- [157] Henrique Weber, Donald Prévost, and Jean-François Lalonde. Learning to estimate indoor lighting from 3d objects. In *International Conference on 3D Vision*, 2018.
- [158] Shuchen Weng, Wenbo Li, Dawei Li, Hongxia Jin, and Boxin Shi. Misc: Multi-condition injection and spatially-adaptive compositing for conditional person image synthesis. In *CVPR*, 2020.
- [159] Huikai Wu, Shuai Zheng, Junge Zhang, and Kaiqi Huang. GP-GAN: Towards realistic high-resolution image blending. In *ACM MM*, 2019.
- [160] Penghao Wu, Li Niu, Jing Liang, and Liqing Zhang.

- Inharmonious region localization via recurrent self-reasoning. In *BMVC*, 2022.
- [161] Penghao Wu, Li Niu, and Liqing Zhang. Inharmonious region localization with auxiliary style feature. In *BMVC*, 2022.
- [162] Zongze Wu, Dani Lischinski, and Eli Shechtman. Fine-grained foreground retrieval via teacher-student learning. In *WACV*, 2021.
- [163] Xuezhong Xiao and Lizhuang Ma. Color transfer in correlated color space. In *ACM international conference on Virtual reality continuum and its applications*, 2006.
- [164] Yazhou Xing, Yu Li, Xintao Wang, Ye Zhu, and Qifeng Chen. Composite photograph harmonization with complete background cues. In *ACM MM*, 2022.
- [165] Dejia Xu, Xingqian Xu, Wenyan Cong, Humphrey Shi, and Zhangyang Wang. Reference-based painterly inpainting via diffusion: Crossing the wild reference domain gap. *arXiv preprint arXiv: 2307.10584*, 2023.
- [166] Ning Xu, Brian Price, Scott Cohen, and Thomas Huang. Deep image matting. In *CVPR*, 2017.
- [167] Ben Xue, Shenghui Ran, Quan Chen, Rongfei Jia, Binqiang Zhao, and Binqiang Zhao. DCCF: Deep comprehensible color filter learning framework for high-resolution image harmonization. In *ECCV*, 2022.
- [168] Su Xue, Aseem Agarwala, Julie Dorsey, and Holly E. Rushmeier. Understanding and improving the realism of image composites. *ACM Transactions on Graphics*, 31(4):84:1–84:10, 2012.
- [169] Binxin Yang, Shuyang Gu, Bo Zhang, Ting Zhang, Xuejin Chen, Xiaoyan Sun, Dong Chen, and Fang Wen. Paint by example: Exemplar-based image editing with diffusion models. In *CVPR*, 2023.
- [170] Raymond A Yeh, Chen Chen, Teck Yian Lim, Alexander G Schwing, Mark Hasegawa-Johnson, and Minh N Do. Semantic image inpainting with deep generative models. In *CVPR*, 2017.
- [171] Jiahui Yu, Zhe Lin, Jimei Yang, Xiaohui Shen, Xin Lu, and Thomas S Huang. Free-form image inpainting with gated convolution. In *ICCV*, 2019.
- [172] Fangneng Zhan, Hongyuan Zhu, and Shijian Lu. Spatial fusion GAN for image synthesis. In *CVPR*, 2019.
- [173] Fangneng Zhan, Shijian Lu, Changgong Zhang, Feiyang Ma, and Xuansong Xie. Adversarial image composition with auxiliary illumination. In *ACCV*, 2020.
- [174] Fangneng Zhan, Jiaying Huang, and Shijian Lu. Hierarchy composition GAN for high-fidelity image synthesis. *IEEE Transactions on cybernetics*, 2021.
- [175] Bo Zhang, Jiacheng Sui, and Li Niu. Foreground object search by distilling composite image feature. In *ICCV*, 2023.
- [176] He Zhang, Jianming Zhang, Federico Perazzi, Zhe Lin, and Vishal M Patel. Deep image compositing. In *WACV*, 2021.
- [177] Jinsong Zhang, Kalyan Sunkavalli, Yannick Hold-Geoffroy, Sunil Hadap, Jonathan Eisenman, and Jean-François Lalonde. All-weather deep outdoor lighting estimation. In *CVPR*, 2019.
- [178] Kaihao Zhang, Wenqi Ren, Wenhan Luo, Wei-Sheng Lai, Björn Stenger, Ming-Hsuan Yang, and Hongdong Li. Deep image deblurring: A survey. *International Journal of Computer Vision*, 130(9):2103–2130, 2022.
- [179] Lingzhi Zhang, Tarmily Wen, Jie Min, Jiancong Wang, David Han, and Jianbo Shi. Learning object placement by inpainting for compositional data augmentation. In *ECCV*, 2020.
- [180] Lingzhi Zhang, Tarmily Wen, and Jianbo Shi. Deep image blending. In *WACV*, 2020.
- [181] Longwen Zhang, Qixuan Zhang, Minye Wu, Jingyi Yu, and Lan Xu. Neural video portrait relighting in real-time via consistency modeling. In *ICCV*, 2021.
- [182] Richard Zhang, Phillip Isola, Alexei A Efros, Eli Shechtman, and Oliver Wang. The unreasonable effectiveness of deep features as a perceptual metric. In *CVPR*, 2018.
- [183] Shengping Zhang, Quanling Meng, Qinglin Liu, Liqiang Nie, Bineng Zhong, Xiaopeng Fan, and Rongrong Ji. Interactive object placement with reinforcement learning. In *ICML*, 2023.
- [184] Shuyang Zhang, Runze Liang, and Miao Wang. ShadowGAN: Shadow synthesis for virtual objects with conditional adversarial networks. *Computational Visual Media*, 5(1):105–115, 2019.
- [185] Song-Hai Zhang, Zhengping Zhou, Bin Liu, Xi Dong, and Peter Hall. What and where: A context-based recommendation system for object insertion. *Computational Visual Media*, 6(1):79–93, 2020.
- [186] Xin Zhang, Jiaxian Guo, Paul Yoo, Yutaka Matsuo, and Yusuke Iwasawa. Subject-driven image editing with pre-trained diffusion model. *arXiv preprint arXiv: 2306.07596*, 2023.
- [187] Hengshuang Zhao, Xiaohui Shen, Zhe L. Lin, Kalyan Sunkavalli, Brian L. Price, and Jiaya Jia. Compositing-aware image search. In *ECCV*, 2018.
- [188] Yanan Zhao, Brian L. Price, Scott D. Cohen, and Danna Gurari. Unconstrained foreground object search. In *ICCV*, 2019.
- [189] Siyuan Zhou, Liu Liu, Li Niu, and Liqing Zhang. Learning object placement via dual-path graph completion. In *ECCV*, 2022.
- [190] Jun-Yan Zhu, Philipp Krahenbuhl, Eli Shechtman, and Alexei A Efros. Learning a discriminative model for the perception of realism in composite images. In *ICCV*, 2015.
- [191] Sijie Zhu, Zhe Lin, Scott D. Cohen, Jason Kuen, Zhifei Zhang, and Chen Chen. GALA: Toward geometry-and-lighting-aware object search for compositing. In *ECCV*, 2022.
- [192] Sijie Zhu, Zhe Lin, Scott Cohen, Jason Kuen, Zhifei Zhang, and Chen Chen. TopNet: Transformer-based object placement network for image compositing. In *CVPR*, 2023.
- [193] Ziyue Zhu, Zhao Zhang, Zheng Lin, Ruiqi Wu, Zhi Chai, and Chun-Le Guo. Image harmonization by matching regional references. *arXiv preprint arXiv:2204.04715*, 2022.
- [194] Zhengxia Zou. Castle in the sky: Dynamic sky re-

placement and harmonization in videos. *arXiv preprint arXiv:2010.11800*, 2020.